



Norwegian  
Meteorological  
Institute

No. 4/2023

ISSN 2387-4201

Meteorology

**METreport**

# **EPS-Sterna constellation impact in regional high-latitude NWP**

Stéphanie Guedj, Harald Schyberg, Máté Mile,  
Per Dahlgren, Roger Randriamampianina

[Classification: free]



<b>Title</b> EPS-Sterna constellation impact in regional high-latitude NWP	<b>Date</b> 24/10/2023
<b>Section</b> Development Centre for Weather Forecasting	<b>Report no.</b> No. 4/2023
<b>Author(s)</b> Stéphanie Guedj, Harald Schyberg, Máté Mile, Per Dahlgren, Roger Randriamampianina	<b>Classification</b> ● Free    ○ Restricted
<b>Client(s)</b> EUMETSAT	<b>Client's reference</b> EUM/CO/22/4600002671/CJA
<p><b>Abstract</b></p> <p>EUMETSAT is presently considering a program for a future constellation of small microwave satellites called EPS-Sterna. It will consist of small-size polar orbiting satellites carrying microwave radiometers providing rapid refresh of observation coverage, particularly dense at high-latitude regions. To help design the mission, EUMETSAT has tasked MET Norway to study the potential impact of EPS-Sterna in the regional NWP AROME-Arctic system.</p> <p>We have built and calibrated an Observing System Simulation Experiment (OSSE), i.e a simulated version of our operational AROME-Arctic system in which three EPS-Sterna constellation scenarios (3 to 6 small satellites on 2 to 3 orbital planes) have been assimilated on top of the existing observing system. We generally demonstrate that the EPS-Sterna constellation is likely to complement the existing observing system well, providing good overall improvements of forecast scores versus the control run. For short forecast ranges (from 3 to 12h) we see pronounced improvements in wind and temperature in the mid troposphere. With regards to existing microwave instruments, in this OSSE, the average relative error reduction expected from EPS-Sterna varies from 3 to 6% for short-range forecasts of humidity, temperature and wind in mid-troposphere. Due to some limiting assumptions made in this OSSE study, this program is expected to have an even larger impact than indicated here.</p>	
<p><b>Keywords</b></p> <p>EPS-Sterna, data assimilation, AROME-Arctic, OSSE, microwave satellite sounding data, high latitudes, observation impact, forecast system</p>	

---

Disciplinary signature

---

Responsible signature

## Executive Summary

EUMETSAT is presently considering a program for a future constellation of small microwave satellites called EPS-Sterna. It will consist of small-size polar orbiting satellites carrying microwave radiometers providing rapid refresh of observation coverage, particularly dense at high-latitude regions. To help design the mission, EUMETSAT has tasked MET Norway to study the potential impact of the EPS-Sterna in the regional NWP AROME-Arctic system.

The future EPS-Sterna constellation would be 1) a good candidate to replace platforms that will not be operational after 2029 and 2) complementary with the sounding services covering nowadays AROME-Arctic, especially its early morning passes. In this study, EUMETSAT supplied the required input to simulate 3 constellation scenarios:

OP3-6SAT : 6 satellites on 3 orbital planes (Baseline scenario)

OP3-3SAT : 3 satellites on 3 orbital planes (Degraded case #1)

OP2-4SAT : 4 satellites on 2 orbital planes (Degraded case #2)

We have built and calibrated an Observing System Simulation Experiment (OSSE), i.e., a simulated version of our operational AROME-Arctic system in which three EPS-Sterna constellation scenarios have been assimilated on top of the existing observing system. Observation errors have been carefully calibrated to ensure the most realistic possible impact of the future EPS-Sterna in the atmospheric analysis and forecast in the Arctic.

Observations have effect both through their usage in data assimilation and through their usage in the host model providing the lateral boundary conditions, where the initial state is more important for short forecast ranges, while the relative impact from the lateral boundaries increases with forecast range. This study assesses the contribution coming from the initial state only. We generally demonstrated that the EPS-Sterna constellation is likely to complement the existing observing system well, providing good overall improvements of forecast scores versus the control run. For short forecast ranges (from 3 to 12h) we see pronounced improvements in wind and temperature in the mid troposphere. With regards to existing microwave instruments, in this OSSE, the averaged relative error reduction expected from EPS-Sterna varies from 3 to 6% for short-range

forecasts of humidity, temperature and wind in mid-troposphere. Due to some limiting assumptions made in this OSSE study, this program is expected to have an even larger impact than indicated here.

# Table of contents

Executive Summary.....	3
1. Background and introduction .....	6
2. The regional NWP system and background on previous impact studies .....	7
2.1 Operational NWP systems in Scandinavia, the AROME-Arctic model and assimilation system.....	7
2.2 Background on previous studies, impact from observation usage in initial state and in lateral boundaries.....	10
2.3 Characteristics of a high-latitude impact study .....	12
3. Potential of EPS-Sterna in AROME-Arctic .....	14
4. Observing System Simulation Experiment setup .....	18
4.1 The usage of the Nature Run .....	18
4.2 Building the OSSEs .....	20
4.3 Common features and expected impacts .....	21
4.4 Microwave observations available in the present observing system.....	22
4.5 Conditions of assimilation.....	23
4.6 Calibration of the observation errors in the OSSE .....	24
4.7 Manual Adjustments and first guess for EPS-Sterna.....	27
4.8 Simulation of EPS-Sterna observations, preprocessing and DA configurations..	29
5. Results .....	32
5.1 Monitoring of active observations and complementarities.....	32
5.2 Impact on the analysis .....	36
5.3 Impact on the forecast.....	41
5.4 Additional “short” experiments and case study.....	44
6. Discussion.....	50
Acknowledgements .....	52
List of Tables and Figures .....	53
References .....	56

# 1. Background and introduction

EUMETSAT is presently considering plans for a future constellation of small microwave satellites based on the upcoming ESA Arctic Weather Satellite. This candidate constellation, EPS-Sterna, will consist of small-size polar orbiting satellites carrying microwave radiometers providing rapid refresh of observation coverage, particularly dense at high-latitude regions. To help design the mission and to assess its potential impact, EUMETSAT has initiated a set of studies with focus from the global to the regional application, where the study described in this report focuses on impact in regional high-latitude Numerical Weather Prediction (NWP). Companion studies focus on global NWP and on nowcasting applications.

While the impact of present components of the observing system for NWP can be assessed with data denial studies (Observing System Experiments, OSEs), assessment of the impact of future observing systems need to rely on a simulation framework. One such framework is the Observing System Simulation Experiment framework (OSSE). See for instance Masutani et al, 2010 and Zeng et al, 2020 for summaries on the methodology and previous studies. This is the method we here use to assess the potential impact of possible EPS-Sterna constellations (see section 4.1 for more details).

We first give an overview of the regional NWP systems used in Scandinavia and their roles in applications by users, including a description of the AROME-Arctic NWP model, which is used in the present study. We also summarise knowledge from existing studies on the impact of various observation types and the impact of observations coming from their use in data assimilation and in providing the lateral boundary fields needed in the regional model. We then present how this OSSE study was set up and present the results seen. We conclude with a discussion on the knowledge that can be extracted from this study along with its limitations.

## 2. The regional NWP system and background on previous impact studies

### 2.1 Operational NWP systems in Scandinavia, the AROME-Arctic model and assimilation system

MET Norway, as well as other European MET services, uses a set of different NWP models forming the basis for their operational forecasting. The models differ not only in their code and formulations, but also in the observations used and in their run schedules and main applications. The regional models need to be fed with forecasts from a global model (host model) on their lateral boundaries. *Table 1* gives an overview of different models used at MET Norway and some characteristics relevant for their usage.

	ECMWF HRES global	MEPS (MetCoOp EPS) /AROME-Arctic	MNWC (MetCoOp Nowcast)
<b>Horizontal resolution</b>	~9 km	2.5 km	2.5 km
<b>Upper-air assimilation</b>	4D-Var EDA	3D-Var	3D-Var with first guess from MEPS
<b>Forecast cycles</b>	6-hourly, 12-hourly main cycles	3-hourly	hourly
<b>Forecast length and output frequency</b>	240h, hourly to 6-hourly output	66h, hourly output	9h, 15 min output
<b>Cut-off time observations for regional NWP</b>		1h 15 min/1h 45 min	25 min
<b>High sampling frequency of ground-based observations</b>		+Ground received GNSS +Weather radar <sup>1</sup>	+Use of sub-hourly GNSS +NetAtmo crowd-sourced obs <sup>2</sup> +Cloud ingest (satellite & SYNOP)
<b>Availability delay to end user</b>	~6 h	~2.5 h	~1 h

*Table 1: Operational models used in forecasting at MET Norway (and other Scandinavian countries).*

<sup>1</sup>GNSS and weather radar are used in MEPS only, not in AROME-Arctic

<sup>2</sup>This refers to the citizen weather stations network measuring various atmospheric variables (<https://www.netatmo.com/>).

Various forecast products from ECMWF are used for long-range forecasting, and forecasts from ECMWF are also used in operations on the lateral boundaries of our regional models. The domains of our main regional models are shown in *Figure 1*. The MetCoOp Ensemble Prediction System (EPS) system (MEPS) is a 30-member ensemble forecasting system which is based on the HARMONIE-AROME code. It covers Scandinavia and surrounding areas, and is run jointly with Sweden, Finland, and Estonia. In addition, MET Norway runs the AROME-Arctic system for forecasting of high-latitude areas, with a very close setup to that of MEPS, but with fewer ensemble members. This is the model used for the present assessments, for this study in its deterministic (non-ensemble) mode.

HARMONIE-AROME is a kilometre-scale, non-hydrostatic model for limited area application. Convection is treated explicitly. The system has been developed with the primary goal of operational regional weather forecasting with intermittent data assimilation. HARMONIE-AROME is based on the shared ALADIN-HIRLAM forecast code framework and is also part of the IFS (Integrated Forecasting System) code framework shared with the ECMWF NWP system. A detailed description of the HARMONIE-AROME model can be found in Bengtsson et al, 2017. AROME-Arctic is an operational implementation of HARMONIE-AROME with adaptation and configurations particularly suited for the Arctic regions, and is described in Müller et al, 2017 and Randriamampianina et al., 2019.

In the 3D-Var assimilation of AROME-Arctic, a fixed climatological background error covariance matrix is used. The statistics were computed using a downscaling technique applied to the IFS ensemble data assimilation (EDA) covering four seasons (i.e., forecast differences from winter, spring, summer, and autumn). The multivariate cross-covariance relationship between vorticity, divergence, temperature and surface pressure, and specific humidity, as described in Berre (2000), is used in this HARMONIE-AROME data assimilation scheme.

The initial conditions for the AROME-Arctic forecasts (i.e., the AROME-Arctic analyses) are updated eight times per day (at 0000, 0300, 0600, 0900, 1200, 1500, 1800, and 2100 UTC) with a 3-hr assimilation cycle. The short-range forecasts (up to 24 hr) discussed in this study are initialised each day of the period of study from the AROME-Arctic 0000 and 1200 UTC analyses.

Through their higher horizontal resolution, MEPS and AROME-Arctic have an advantage in the description of small-scale phenomena compared to the global ECMWF HRES system. They are also run with relatively short cut-off times for observations (the time after a forecast base time it waits for observations), allowing forecasts to be delivered about 2.5 hours after the base time, much faster than the 6 hours for ECMWF HRES, thus providing forecasts based on fresher observations. The systems are also different in the parts of the observing system they exploit. ECMWF has a more advanced assimilation system (4D-Var EDA), exploiting a large range of observation types, while MEPS and

AROME-Arctic run 3D-Var systems. The regional systems of MEPS exploit some high sampling frequency observation types not used in the global system as indicated in *Table 1*.

In addition to the MEPS and AROME-Arctic suites, we also run a METCoOp Nowcasting NWP suite (MNWC), with even shorter observation cut-off time and hourly forecast production, which uses even more high-frequency observation types than in the other systems. This system with more frequent cycling also benefits from high-frequent ground based GNSS observations, high-frequent NWCSAF based cloud-fraction, cloud-top and temperature and high-frequent crowd-sourced temperature observations. MetCoOp Nowcast assimilates observations with hourly frequency. The model cycling (hourly) is the current operational limit for how frequent observations are used, while the observation input to MNWC itself is sub-hourly for several of the sources. The high density and frequent coverage of EPS-Sterna could be very relevant for such nowcasting NWP systems as well.

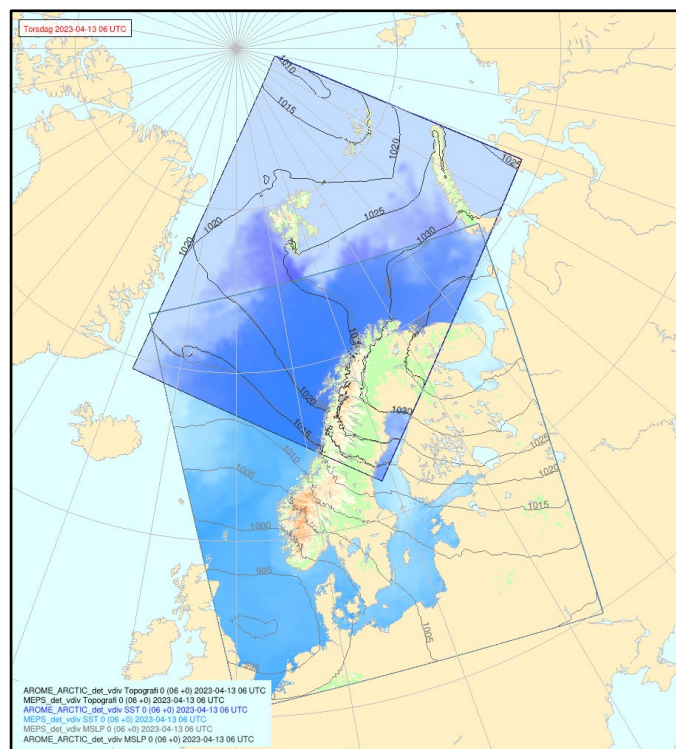


Figure 1: The AROME-Arctic domain (upper rectangle) together with the MetCoOp EPS domain

Through enhancing the possibility of rapid refresh of microwave observation coverage, an EPS-Sterna constellation will be a particularly relevant observing system for improving regional models as described here. We here look into its potential use in the AROME-Arctic system, even if it is possible that there could be an even larger usefulness in a system like MNWC.

## 2.2 Background on previous studies, impact from observation usage in initial state and in lateral boundaries

Several studies in global NWP have demonstrated satellite radiances to be a backbone of the NWP observing system. In particular, global studies show a significant impact on forecast quality coming from the total contribution of the many polar orbiting satellites carrying microwave radiometers providing temperature and moisture profile related information (Lawrence et al., 2019). Such impact has also been confirmed in studies in limited-area models, including over Arctic areas. Here infrared satellite radiances have been demonstrated to be the satellite system giving most impact, while microwave radiances have been shown also to be important, in particular for the moisture verification (Randriamampianina et al, 2019). As shown from Randriamampianina et al (2019) in *Figure 2*, IASI together with radiosounding observations are the two observing systems providing the maximum impact in the atmospheric analysis. With significantly fewer observations, microwave data also shows quite a strong impact in the analysis following the Degree of Freedom for Signal (DFS) diagnostic. It should also be noted that in such a regional model domain, the available observation coverage varies strongly throughout the day.

The various observation types have effect both through their usage in data assimilation and through their usage in the host model providing the lateral boundary conditions. The data assimilation providing the initial state is more important for short forecast ranges, while the relative impact from the lateral boundaries increases with forecast range. Randriamampianina et al, 2021, was the first observing-system experiment study where the relative impact of observations on a regional NWP system gained through lateral boundary conditions (LBCs) was quantified along with the impact from assimilation within the regional model. This study was also based on the AROME-Arctic model. In *Figure 3*, Randriamampianina et al, 2021 showed that microwave data assimilated in regional NWP had a maximum impact on short-range forecast (up to 24h) and close to the surface. After 24 hours, microwave data that had been assimilated in the global system became the dominant impact in the long-range forecast skills of the regional system.

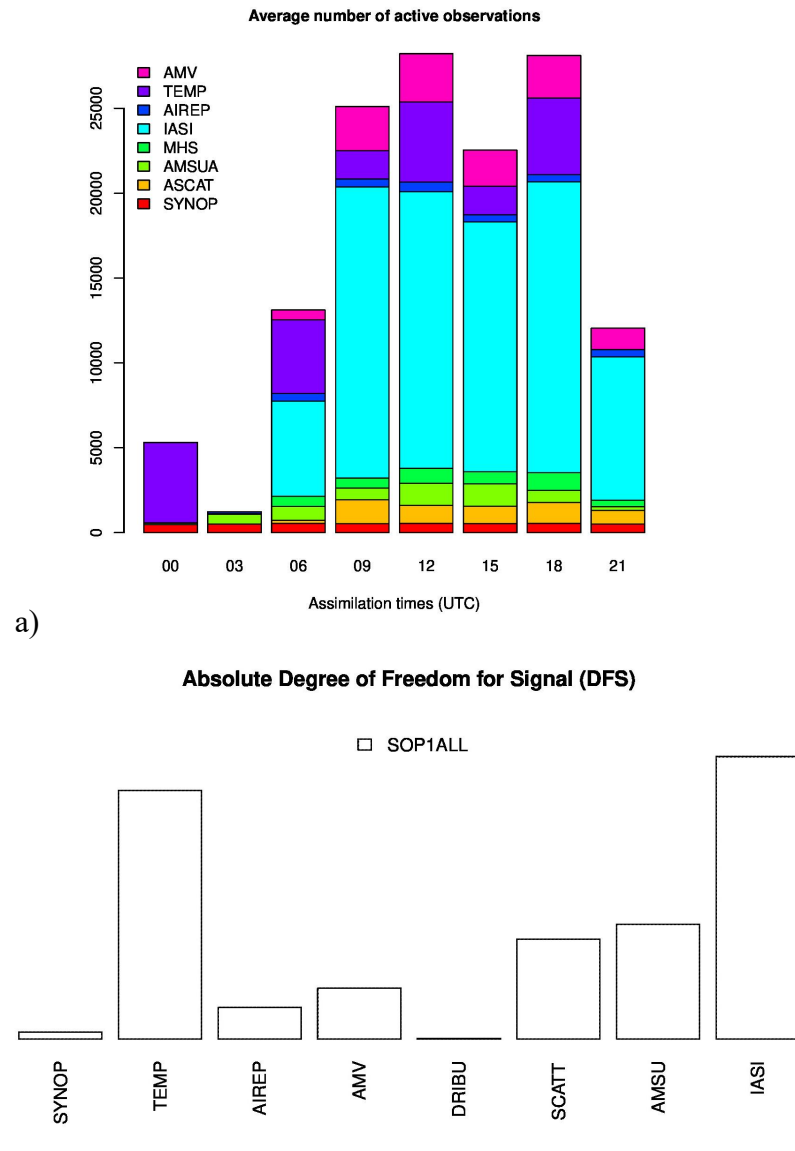


Figure 2: a) Average number of active observations in AROME-Arctic for each assimilation cycle (10 days averaged number of actively assimilated observations) and b) absolute Degree of Freedom for Signal (DFS) for each observation type (averaged over 4 distant assimilation time), (from Randriamampianina et al, 2019).

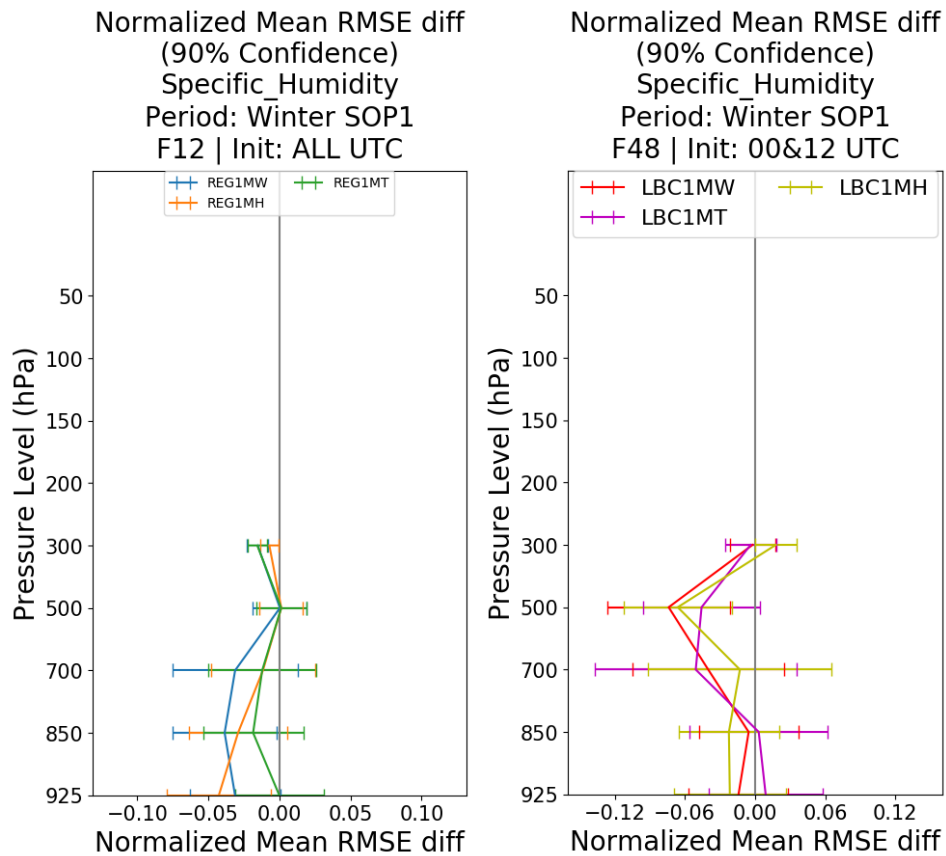


Figure 3: Difference in mean RMSE, normalized by the mean scores for 12- and 48-hr forecasts of specific humidity, between the 2 experiments in which all observations are used and various experiments in which conventional and satellite observations are denied from the regional DA. The impact of microwave (MW) observations, Humidity channels (MH) or Temperature channels (MT) through regional (REG, left panel) DA or through lateral boundary conditions (LBC, right panel) is thus shown in per cent (e.g., from  $-12$  to  $12\%$ ). Negative/positive values indicate positive/negative impact of observations on forecast skill. A 90% two-sided statistical significance test is applied, and verification is against the eight radiosonde stations in the AROME-Arctic domain. From Randriamampianina et al, 2021, more details provided there.

Following these results, EPS-Sterna is in the present study setup expected to show its maximum impact on the short-range forecast (up to 24 hours) of AROME-Arctic. In this context, one can also assume to obtain a larger and significant impact on long-range forecast when EPS-Sterna will be also assimilated in the ECMWF forecast system as it will be used as the LBC.

### 2.3 Characteristics of a high-latitude impact study

Since this study focuses on the impact of an EPS-Sterna constellation in a high-latitude limited-area, AROME-Arctic, it is of interest to underline some characteristics of observation coverage in such a region, which is of relevance to observation impact assessments. The complementarity between polar platforms coverage and the added value of EPS-Sterna is discussed below in section 3.2. This region contains large, relatively remote areas with limited coverage of conventional observations (Figure 4). The satellite

observing system, and in particular polar orbiting satellites, play a relatively larger role in such areas, and satellite observations will to a less degree “compete” with conventional observations, thus satellite information has a relatively larger impact. Also, the tracks of polar orbiting satellites will be denser at high latitudes. This means that the density of other satellite data, with which EPS-Sterna will “compete”, will be larger, but on the other hand, the density of EPS-Sterna orbit tracks will as well be denser than at lower latitudes.

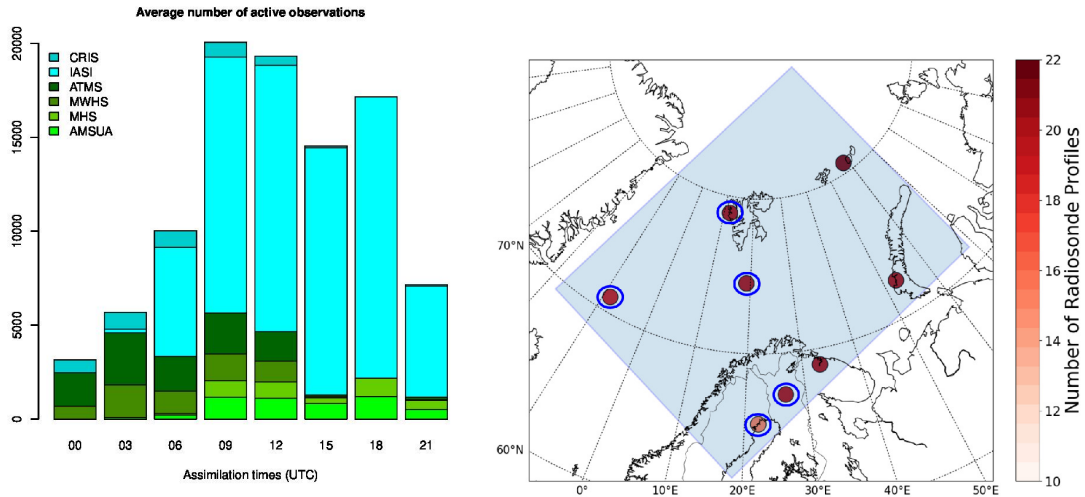


Figure 4: Average number of active satellite observations in AROME-Arctic for each assimilation cycle (10 days averaged number of actively assimilated observations), from Randriamampianina et al, 2021.

In summary, the impact of the total satellite observing system in such a domain is expected to be higher than in European areas further south. We can also expect to get an impression of the impact of EPS-Sterna relative to that of other polar orbiting observations which is also relevant for areas at lower latitudes. This can however also be subject to saturation effects, if the density of satellite observations is so high that there are few gaps left to fill, causing any impact of additional observations to be limited. The density of satellite observations will be expected to be further from saturation at lower latitudes.

### 3. Potential of EPS-Sterna in AROME-Arctic

Based on the Arctic Weather Satellite (AWS) currently developed by the European Space Agency (ESA), EUMETSAT is considering operating EPS-Sterna, a constellation of polar orbiting microwave sounders on small satellites. If materialised, the EPS-Sterna program would provide an unprecedented amount of observations relevant to improve regional forecasting and nowcasting at high latitudes.

Each small satellite will carry a microwave sounder with a 19-channel microwave sounding instrument (*Table 2*), to provide cross-track scanning temperature and humidity sounding capabilities in the 50, 183, and 325 GHz bands.

Channel		Central frequency (GHz)	Bandwidth (MHz)	NEAT	Polarisation	Resolution
Name	index					
Sterna-11	1	50.3	180	< 0.6 K	QV	≤ 40 km
Sterna-12	2	52.8	400	< 0.4 K	QV	≤ 40 km
Sterna-13	3	53.246	300	< 0.4 K	QV	≤ 40 km
Sterna-14	4	53.596	370	< 0.4 K	QV	≤ 40 km
Sterna-15	5	54.4	400	< 0.4 K	QV	≤ 40 km
Sterna-16	6	54.94	400	< 0.4 K	QV	≤ 40 km
Sterna-17	7	55.5	330	< 0.5 K	QV	≤ 40 km
Sterna-18	8	57.290344	330	< 0.6 K	QV	≤ 40 km
Sterna-21	9	89	4000	< 0.3 K	QV	≤ 20 km
Sterna-31	10	165.5	2800	< 0.6 K	QV	≤ 10 km
Sterna-32	11	176.311	2000	< 0.7 K	QV	≤ 10 km
Sterna-33	12	178.811	2000	< 0.7 K	QV	≤ 10 km
Sterna-34	13	180.311	1000	< 1 K	QV	≤ 10 km
Sterna-35	14	181.511	1000	< 1 K	QV	≤ 10 km
Sterna-36	15	182.311	500	< 1.3 K	QV	≤ 10 km
Sterna-41	16	325.15±1.2	2*800	< 1.7 K	QV	≤ 10 km
Sterna-42	17	325.15±2.4	2*1200	< 1.4 K	QV	≤ 10 km
Sterna-43	18	325.15±4.1	2*1800	< 1.2 K	QV	≤ 10 km
Sterna-44	19	325.15±6.6	2*2800	< 1 K	QV	≤ 10 km

*Table 2: EPS-Sterna channel list and characteristics applicable this study*

The future EPS-Sterna constellation would be 1) a good candidate to mitigate the loss of microwave platforms that will not be operational after 2029 and 2) complementary with the sounding services covering nowadays AROME-Arctic, especially its early morning passes. As shown in *section 2.2* and discussed in *section 4.2*, the actual coverage is presently far from optimal. Only two assimilation windows (09 UTC and 12 UTC) benefit from full and dense enough coverage from microwave observations to constrain the atmospheric analysis of temperature and humidity. AMSU-A and MHS are assimilated at high resolution, every 80km. MWHS-2 and ATMS, being still in monitoring mode in AROME-Arctic at the time this study started, are assimilated every 125 km in this study. MWHS-2 is now assimilated at high resolution in the operational AROME-Arctic system. ATMS being still only disseminated to our centre as superobbing, it is technically not possible to increase the resolution.

EUMETSAT supplied the required input to simulate 3 constellation scenarios:

- OP3-6SAT : 6 satellites on 3 orbital planes (Baseline scenario)
- OP3-3SAT : 3 satellites on 3 orbital planes (Degraded case #1)
- OP2-4SAT : 4 satellites on 2 orbital planes (Degraded case #2)

	<b>Orbital Plane &amp; Satellite number</b>	<b>Relative phase in the orbits (degrees)</b>
<b>OP2-4SAT</b>	P1S1	0000
	P2S1	0090
	P1S2	0180
	P2S2	0270
<b>OP3-3SAT</b>	P1S1	0000
	P2S1	0120
	P3S1	0240
<b>OP3-6SAT</b>	P1S1	0000
	P2S1	0060
	P3S1	0120
	P1S2	0180
	P2S2	0240
	P3S3	0300

*Table 3: Orbital plane and satellite number associated to relative phase in the orbits (Walker constellation criteria)*

As shown in *Table 3* satellites have a different starting position on the respective plane relatively to the first satellite that occupies the first place. Following the criteria of a Walker constellation, this shift is supposed to provide the best area coverage within a given time frame. Consequently, the starting positions of the satellites depend on both the orbital plane and the satellite numbers. Local Time of the Descending Node (LTDN) has been stated to 3:30 UTC, 11:30 UTC and 7:30 UTC for P1, P2 and P3 respectively.

All the necessary information to simulate the radiances were provided by EUMETSAT in binary files, each covering 6 hours. Each binary file was converted to ASCII files to extract time/geolocation information, viewing geometry, expected sample noise per channel, etc. *Figure 5* shows an example of EPS-Sterna covering the 15 UTC assimilation window (+/-1 hour and 30 minutes) over Pan-Arctic region.

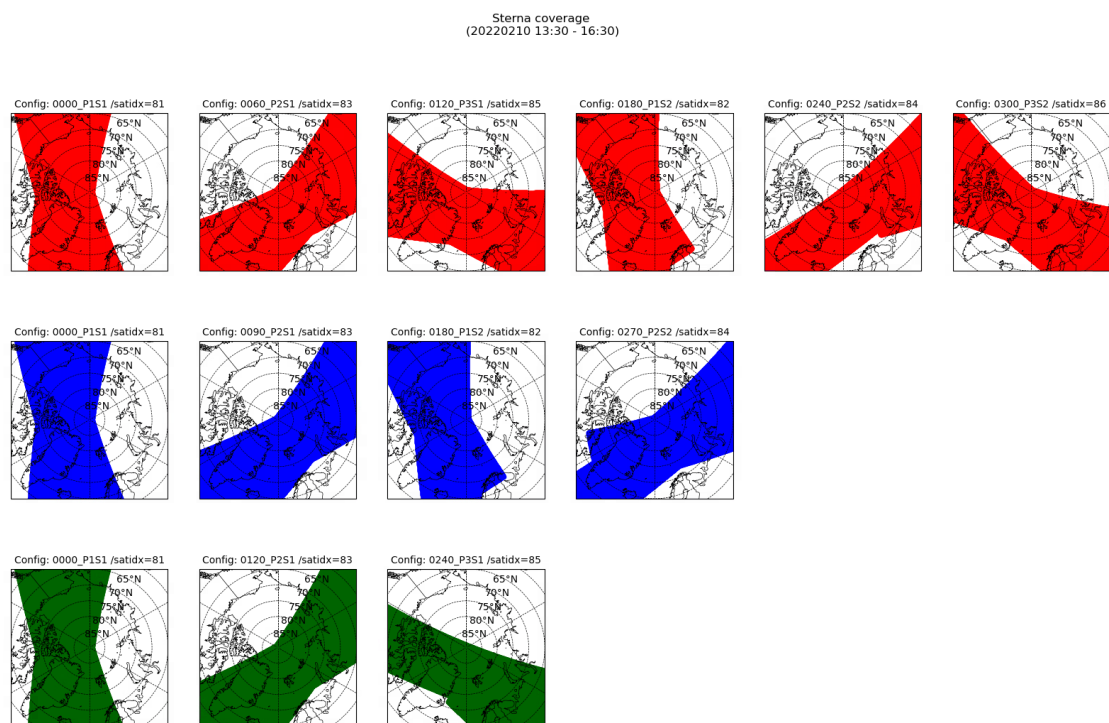


*Figure 5: Example of EPS-Sterna coverage over Arctic for the 3 configurations (OP3-6SAT in red, OP2-4SAT in blue and OP3-3SAT in green) for the assimilation window of 15 UTC (+/-1 hour and 30 minutes).*

In the binary files, it was assumed that all channels have the same geolocation of about 100 km distance which is slightly below its foreseen future performances. With regards to other sounders that are assimilated at a higher resolution, one might expect an underestimated impact of EPS-Sterna.

EPS-Sterna will carry sounders that have similar channels to existing instruments (*Figure 6*). High peaking temperature and humidity channels have been shown to have a positive impact in the Arctic (Lawrence, 2019, Lindskog et al, 2021, and Randriamampianina et al, 2021). Low-peaking channels data assimilation requires a good knowledge of the

surface temperature and emissivity. In AROME-Arctic, surface-sensitive microwave observations are operationally assimilated over land and sea-ice using the so-called dynamic emissivity method (Karbou et al., 2006). This method has been recently applied to ATMS and MWHS-2 instruments in operations, showing positive impact on the forecast skills close to the surface. However, in the present OSSE framework this dynamic emissivity method was not yet implemented and could not be used for this study.

In order to be consistent with other instruments and our experiences in AROME-Arctic, this study considers the assimilation of 50GHz's temperature channels from 3 to 8 and 180GHz's humidity channels from 11 to 15. This study does not cover the 325GHz's group of channels due to a lack of time and experience with these frequencies. To our knowledge, no NWP centre has evaluated the potential of the radiance assimilation of these channels yet. In addition, we had to keep a conservative approach for EPS-Sterna and blacklist the low-peaking channels over land and sea-ice. However, one can refer to the ESA AWS preparation project where this aspect will be covered (ongoing work, report to be published).

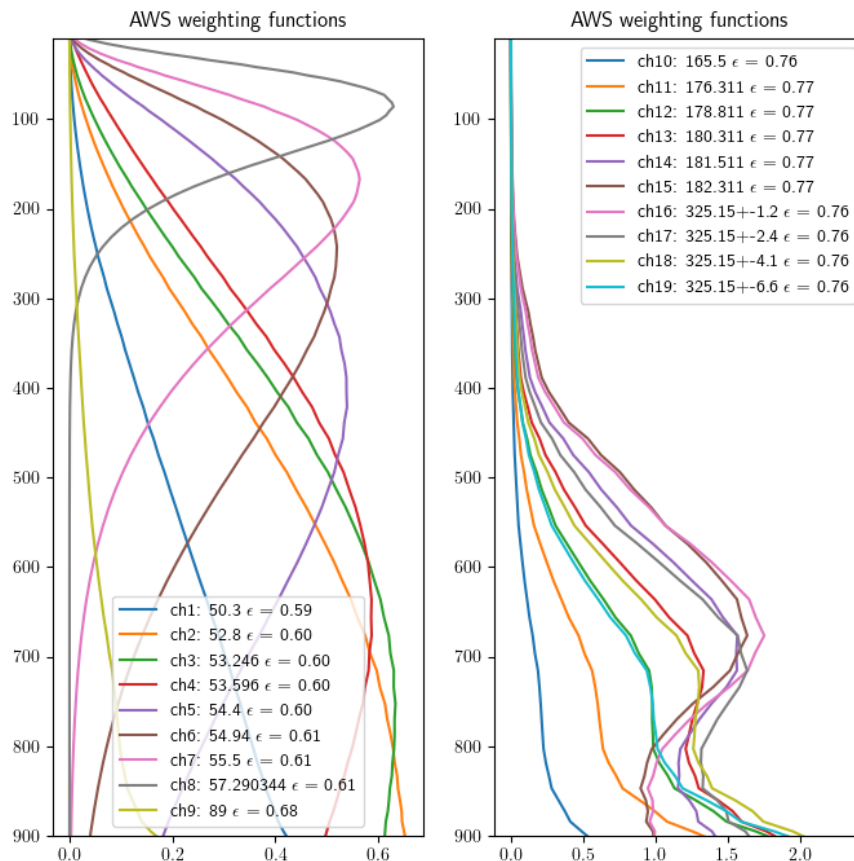
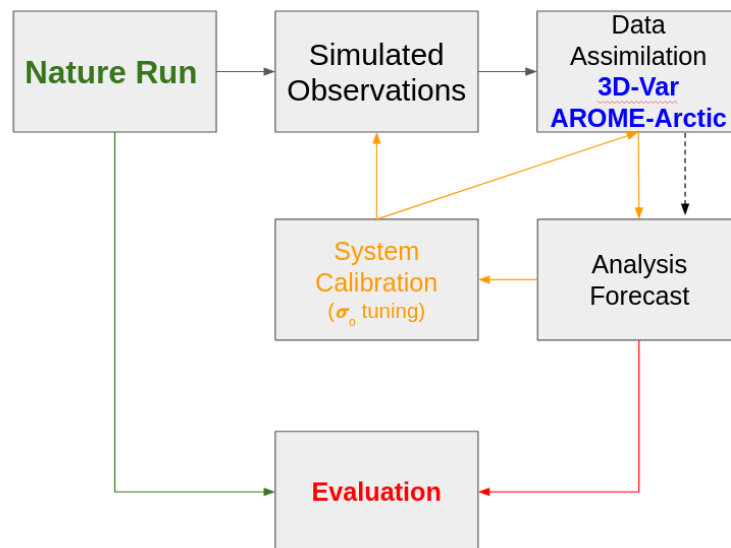


Figure 6: AWS weighting function assuming a standard atmosphere, applicable this study of EPS-Sterna (source: ESA-Sterna project - Adam Dybbroe).

## 4. Observing System Simulation Experiment setup

### 4.1 The usage of the Nature Run

OSSEs are complex and powerful tools, however computation demanding, to assess the impact of a future instrument in NWP systems. It consists in running data assimilation (DA) and forecast experiments in which simulated observations are used instead of real observations. Observations in OSSEs are simulated by using the assumed “true” state of the atmosphere coming from a global and free-run forecast run (called the Nature Run) as input to forward operators and adding simulated errors with appropriate statistical properties. The full organisation of the OSSE is illustrated in *Figure 7*.



*Figure 7: Organisation of the Observing System Simulation Experiment*

Since the ‘true’ state of the atmosphere, here the Nature Run, is perfectly known, the regional OSSE framework allows evaluation of the impact of observations from the potential configurations of an EPS-Sterna constellation on analysis and forecast skill in AROME-Arctic, keeping in mind that results might be influenced by the imperfections and limitations of the OSSE system.

The OSSE we built at MET Norway uses a Nature Run provided by Météo-France. They were willing to share their Nature Run used in their parallel EPS-Sterna study for EUMETSAT with the ARPEGE global model.

The global atmospheric fields from ARPEGE were available every 3-hour, on 115 levels and were used for:

- 1) simulating “true” observation values, before adding simulated observation errors;
- 2) initial first guess for spin-up period, surface conditions and lateral boundary conditions for the AROME-Arctic regional model;
- 3) verification and impact study.

*Figure 8* shows an example of the surface temperature field extracted from the Nature Run and interpolated on the AROME-Arctic domain.

Ideally, the lateral boundary should be perturbed to introduce some uncertainties scaled on those from the ECMWF forecast system to better mimic our AROME-Arctic system. This should be done principally because the lateral boundaries very quickly affect the interior of the regional model solution. The use of perfect boundary conditions from the Nature Run unrealistically constrains the long-range forecast (Errico and Baumhefner 1987; Denis et al. 2002). As discussed in section 2.2, the impact of assimilated observations in the global run of IFS used as boundary conditions has been shown to be dominating the forecast skills of AROME-Arctic after 24h (Randriamampianina et al, 2021). Following this result the OSSE has been run up to 24h forecast.

In addition, because the impact of microwave observations is large on the low levels of the atmospheric analysis and forecast of humidity, one should consider performing surface data assimilation with perturbed observations simulated from the Nature Run. Due to lack of time and computing resources, the surface assimilation was run using the Nature Run fields (including SST) and perfect observations, forcing the surface variables towards a “perfect state” with unrealistically small errors. In addition, only clear-sky assimilation was performed (both for MW and IR data), as it is done in our AROME-Arctic operational system.

As a result, this limitation will imply a significant under-estimation of the impact of EPS-Sterna that could have propagated toward the surface via 1) the structure function of the background matrix and 2) the assimilation of low-peaking channels over land and sea-ice. The decision not to assimilate those channels is further discussed later in this report.

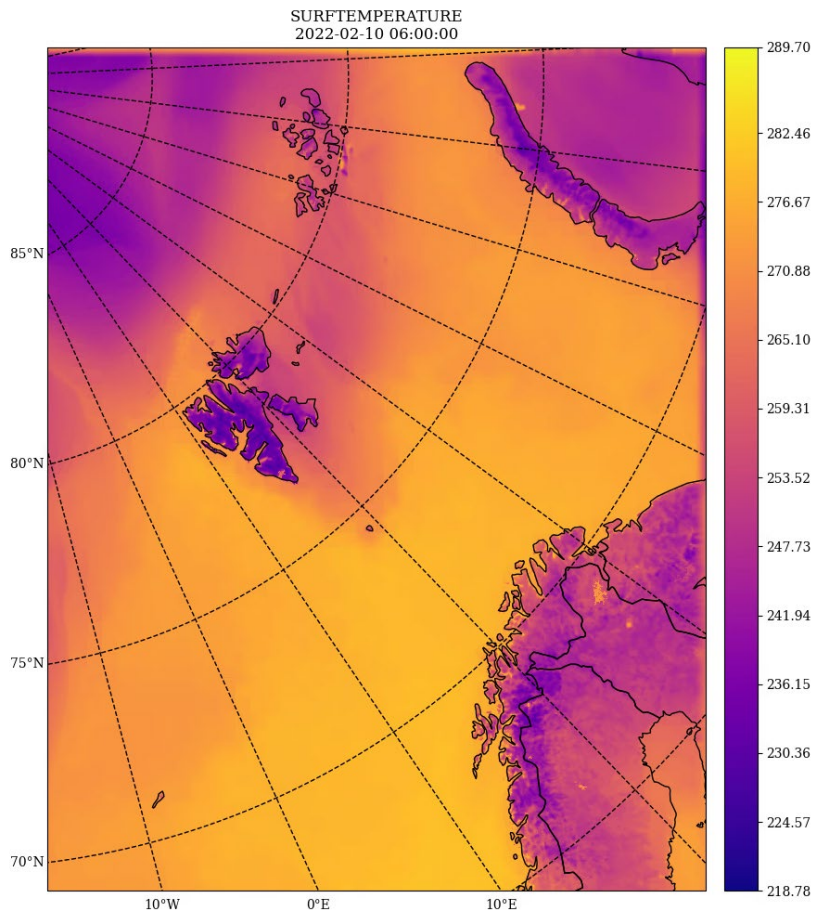


Figure 8: Example of the surface temperature field extracted from the Nature Run and interpolated on the AROME-Arctic domain on the 10/02/2022 at 06 UTC.

## 4.2 Building the OSSEs

Two initial sets of experiments were run to build and calibrate the OSSE called the “real world” and the “simulated world”.

**The “real world” experiment** is a simplified version of the operational AROME-Arctic system (cy43 - newly installed on the ECMWF supercomputer facility called ATOS), using real observations and lateral boundary conditions (LBC) from IFS. It was run for 2 months in winter (January and February 2022) and 2 months in summer (August and September 2021).

This version of AROME-Arctic uses the same set of radiance data as the operational run: AMSU-A, MHS and IASI together with the sparse network of conventional observations (e.g., surface, aircraft, radiosonde, drifting buoys, ship). MWHS-2 and ATMS instruments being both in pre-operational mode (when the study started, but operational since February 2023) are also used in this study at a different thinning distance. Unlike the operational setup, scatterometer (ASCAT) and atmospheric motion vector (AMV)

wind data were discarded from the 3D-Var assimilation system. The justification for it is given further down in the description of the “simulated world” experiment.

The LBC update frequency coming from ECMWF IFS was reduced to 3 hrs, compared with hourly in the setup used for operational AROME-Arctic forecasts, to reduce the (archiving) cost of both global and regional experiments and be consistent with the way the Nature Run is used as LBC in the “simulated world”. The surface assimilation is based on the SURFEX software (Masson et al., 2013) to compute the surface initial state from optimal interpolation between a short-range forecast and surface observations (including 2m measurements). Over ocean, the SST is provided by the IFS LBC.

**The “simulated world” experiment** has a similar setup of the “real world experiment”. However, instead of using real observations and LBC from IFS, this configuration assimilates simulated observations and the LBC generated from the Nature Run available every 3 hours.

The set of radiance observations that were simulated was the same as the one in the “real world experiment” (AMSU-A, MHS, IASI, ATMS and MWHS-2). Since the AMV and ASCAT observations are indirect measurements of winds (level 2 product), a specific observation operator should have been implemented to retrieve these qualities based on the Nature Run state and not the real state of the atmosphere. This might be considered in a further study. In addition, the Nature Run together with unperturbed observations were used to force the boundary conditions at the surface.

### **4.3 Common features and expected impacts**

For simulating and assimilating radiances, the same RTTOV radiative transfer model (RTM) was used (version 11.2). Atmospheric profiles together with surface temperature variables were extracted from the previous 3h-forecast in the real world and from the Nature Run in the “simulated world” and used as input into the RTM. The emissivity was provided from the FASTEM model (Lui et al., 2011) over ocean for all existing instruments. Over land and sea-ice, the so-called dynamic emissivity (Karbou et al., 2006) was used for existing instruments in both “worlds”. For EPS-Sterna, emissivity was computed from the classification-based model from Weng et al. (2001). Uncertainties of the latter constrained us to blacklist surface-sensitive channels for EPS-Sterna. Other needed information such as the timing and locations of individual observations and the observing geometry (scan angle and Earth incidence angle) were extracted from the real observation BUFR file or the HARMONIE-AROME diagnostic file output. To simulate the future EPS-Sterna constellations, EUMETSAT has provided such information for various scenarios of the constellation (see section 3). The handling of EPS-Sterna radiances mimics what was done for existing microwave sounding instruments, in particular AMSU-A and MHS, with adaptations for the frequency channels planned for EPS-Sterna.

In addition to radiances, the operational AROME-Arctic system uses a sparse network (in this region) of conventional data such as aircraft, radiosondes, buoys, surface pressure. Conventional observation data are interpolated directly from the Nature Run — no forward calculations are required. In the same way as radiances, the needed information regarding time, location and geometry were extracted from the real observation files at the corresponding time.

Ideally, the observation operators used in the data assimilation system should be different from those used to generate the synthetic observations so that realistic representativeness error is introduced. We assumed here that a sufficient representativeness error was indirectly brought by the difference in horizontal resolution between the Nature Run and the AROME-Arctic forecast system, and partly implicitly by adjustment of the assumed observation errors in the calibration procedure described in Section 4.5 below.

#### 4.4 Microwave observations available in the present observing system

Assimilation in AROME-Arctic is done three-hourly, and the coverage of microwave observations varies throughout the day. Presently, in the operational version of AROME-Arctic, observations from MHS (onboard Metop-B and -C), AMSU-A (onboard NOAA-19, Metop-B and -C), ATMS (on NPP and NOAA-20), MWHS-2 (onboard FY-3D) are actively assimilated together with IASI and conventional data. The averaged amount of active microwave observation per channel is presented in *Table 4*.

This is of relevance for the expected impact of new observations, to what extent they “compete” with other observations and to what extent they fill gaps.

UTC	00	03	06	09	12	15	18	21
N obs	70	160	240	1020	930	590	920	220

*Table 4: Averaged amount of active microwave observations without EPS-Sterna per (high peaking) channel over a month (February 2022).*

In *Figure 9* we present typical coverage of passive microwave sounding observations in our domain, which are relevant as they provide information of similar type as EPS-Sterna. We see that we have a very good coverage in the present observing system already on several of the times of the day, while on other times the total coverage is less complete. In particular there seems to be a potential for improved coverage at 21 UTC, 00 UTC, 03 UTC and 06 UTC. The different thinning distance applied to ATMS and MWHS-2 has been discussed in the previous section.

## Coverage of microwave observations in AROME-Arctic (Oper)

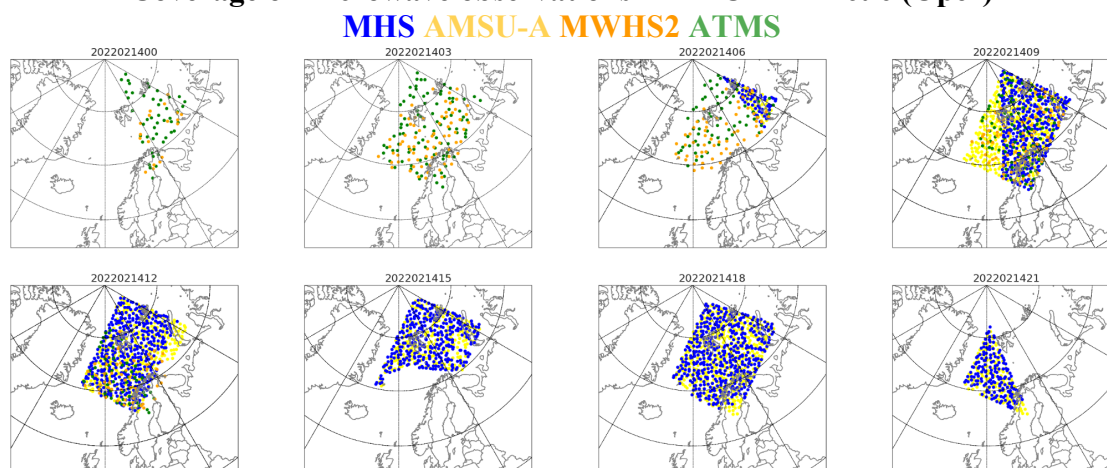


Figure 9: Example coverage of existing (high peaking) passive microwave sounding data used in the assimilation in the AROME-Arctic domain, on 14 February 2022: MHS (blue), AMSU-A (yellow), MWHS-2 (orange) and ATMS (green).

### 4.5 Conditions of assimilation

	Active channels	Freq. (GHz)	Type of sounding	Observations assimilated over:
<b>AMSU-A</b>	5-9	50	Temperature	ch5-6: Ocean ch7-9: Land, ocean, sea-ice
<b>MHS</b>	3-5	183	Humidity	ch3-4: Land, ocean, sea-ice ch5: Ocean
<b>ATMS</b>	6-9	50	Temperature	ch6: Ocean ch7-9: Land, ocean, sea-ice
	19-22	183	Humidity	Land, ocean, sea-ice
<b>MWHS-2</b>	2-6	118	Temperature	Land, ocean, sea-ice
	11-12	183	Humidity	Land, ocean, sea-ice

Table 5: Adjustment of the conditions for microwave data assimilation in the OSSE

Since EPS-Sterna will not use dynamic emissivity methods to assimilate the low-peaking channels over land (Karbou et al, 2006), it was decided to apply the same strategy to other instruments and update the blacklist accordingly.

## 4.6 Calibration of the observation errors in the OSSE

Calibration of OSSEs verifies the simulated data impact by comparing it to real data impact. To conduct an OSSE calibration and to build the control run, the data impact of each existing instrument has to be compared to their impact in the OSSE. To ensure that the OSSE behaves realistically in the analysis and short-range forecast, first-guess and analyses departures from the “simulated world” have to match these from the “real world”.

These statistics are partly determined by the statistics of observation errors, as revealed by the fundamental data assimilation equations. Also known as measurement error or observational uncertainty  $\sigma_o$ , this quantity refers to the uncertainty associated with the measurements or observations. It includes several sources of uncertainties: instrument error, sample error, bias, random error, interpolation error and representativeness error. *Figure 10* gives the first estimates of microwave brightness temperature observation errors (before calibration) as set in AROME-Arctic.

It is a common practice in most NWP centres to significantly overestimate these errors with regards to the instrument noise itself in order to account for other sources of uncertainties. In the framework of this OSSE, the calibration of observation error (denoted  $\sigma_o$  hereafter) has been done in 2 steps:

- Overall calibration: pre-tuning all satellite at once  $\sigma_o$
- Manual adjustments of observation error for microwave instruments

Any change in the observation error induces a set of experiments:

- 1) Create perfect observations and allocate the prescribed observation error in the observational database (ECMA)
- 2) Run offline a procedure (“Pertobs.F90”) to generate perturbed observations: Add random noise scaled on the prescribed observation error. Errors are assumed to be uncorrelated.
- 3) Assimilation experiment of simulated and perturbed observations for 10 days
- 4) Evaluation of the fit between analysis/FG departures from “simulated world” and “real world”.
- 5) Adjust the perturbation and restart from 1)

## Overall Calibration

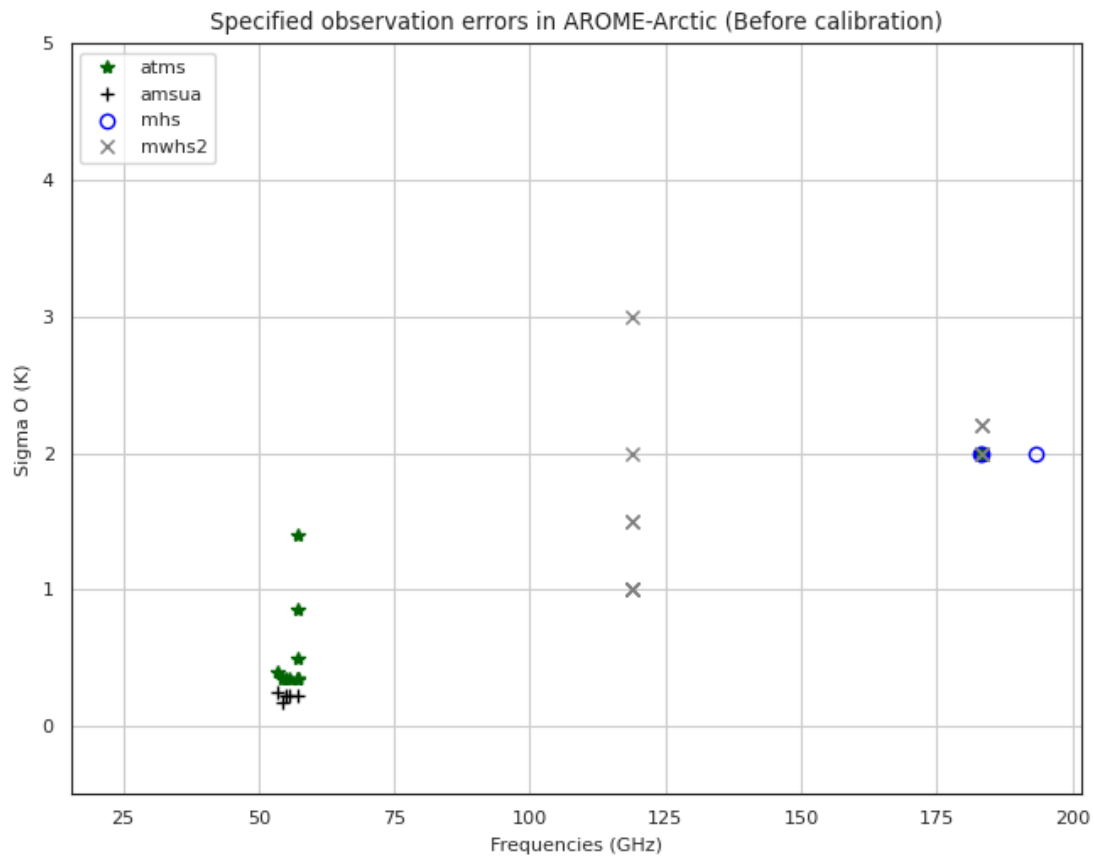


Figure 10: Specified observation errors in AROME-Arctic for microwave instruments (before calibration)

There is a variable called SIGMAO\_COEFF in the code, allowing to tune the specified observation error from all satellite instruments at the same time. By default, this coefficient is set to 1 in the “real world”. 5 scenarios of coefficients have been tested: 1.1, 0.9, 0.7, 0.5 and 0.2, increasing or decreasing the specified observation error. Figure 11 shows an example of analysis departures histograms at AMSU-A sounding channels assimilated with different scenarios of SIGMAO\_COEFF. *Oper* refers to the “real world” settings. The naming *osse0p2*, *osse0p5* and *osse0.7* refer to SIGMAO\_COEFF at 0.2, 0.5 and 0.7 respectively. In order to ensure the assimilation of AMSU-A channel 8 and 9 in the “simulated world” has a similar impact as in the “real world”, Figure 11 indicates that the specified observation error of that channel should be reduced by about 50%. This exercise has been done for each observation type of the OSSE. Another example is given with MHS channel 3 in Figure 12 to illustrate the effect of calibration on first guess departures of humidity channels.

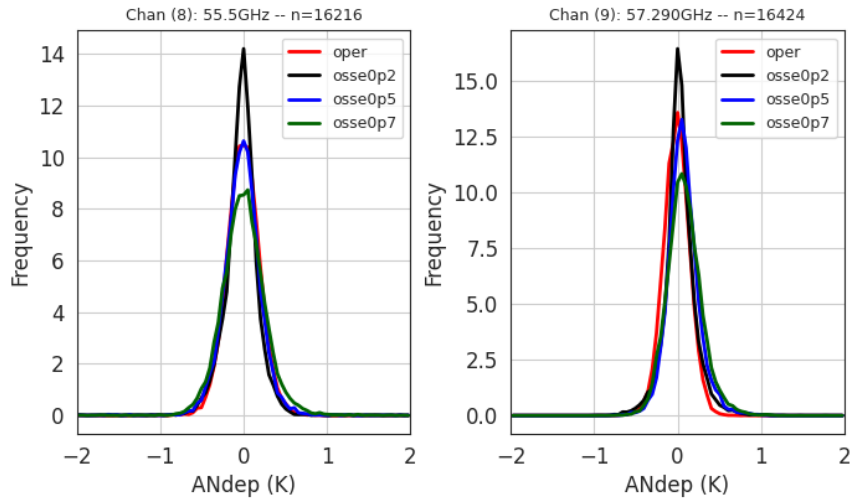


Figure 11: Frequency histograms of analysis departures to observations (in K) at AMSU-A channel 8 and 9 using different scenarios of observation errors. Oper refers to the “real world” settings. osse0p2, osse0p5 and osse0.7 refer to SIGMAO\_COEFF at 0.2, 0.5 and 0.7 respectively.

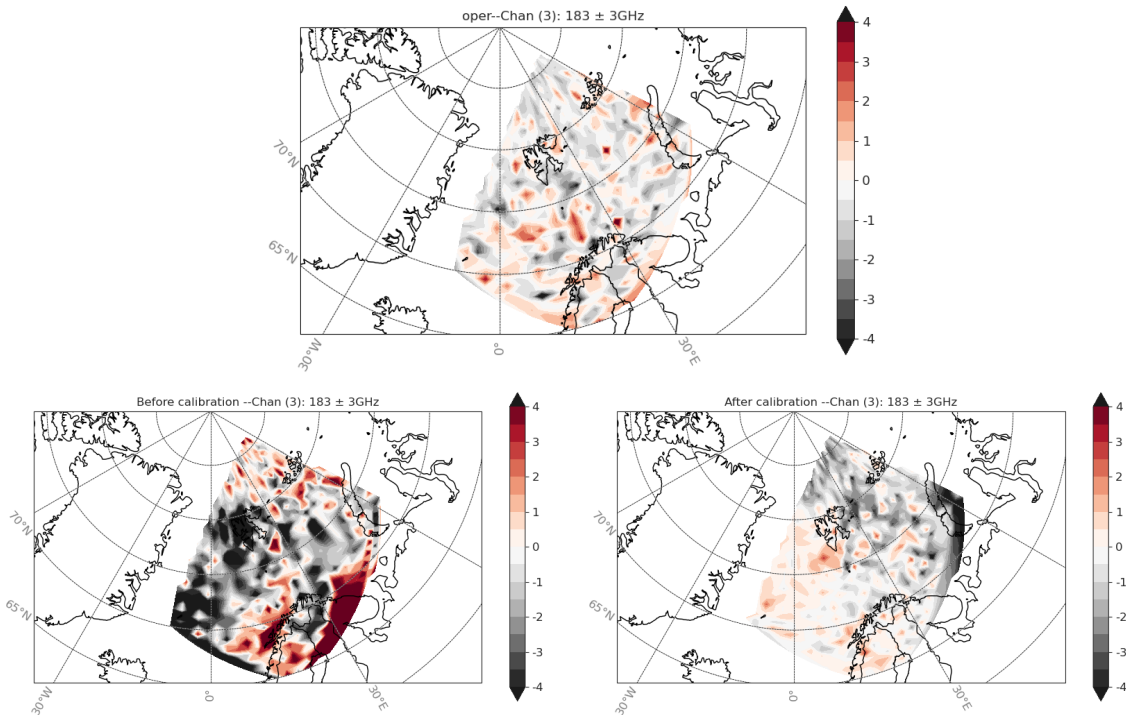


Figure 12: Maps of first guess departure to MHS channel 3 observations in the “real world” (upper line) compared to those from the uncalibrated (bottom, left panel) and calibrated (bottom, right panel) “simulated world”.

The overall calibration suggested a reduction of about 80% of satellite observation errors for most of the humidity channels and a reduction of about 50% for temperature channels with regards to the default value implemented in the operational system. As expected, in most cases, the suggested observation error is close to the actual instrument error, neglecting other sources of uncertainties that are applicable only in the “real world”. It

was found that for radiosondes, aircraft and synop data, observation errors could be reduced by about 10%.

#### 4.7 Manual Adjustments and first guess for EPS-Sterna

Following the overall calibration, observation errors for microwave observations have been further refined, channel by channel. Special attention has been given to the calibration of existing microwave instruments because we want to assess the impact of EPS-Sterna vis-à-vis the other microwave instruments.

Figure 13 shows the impact of the overall tuning (before in black and after in green) and the effect to manually adjust the observation errors on first guess departures to ATMS radiances (dotted green line). The match between statistics in the “simulated world” and the “real world” is greatly improved which ensures that the OSSE behaves realistically in the analysis and short range forecast.

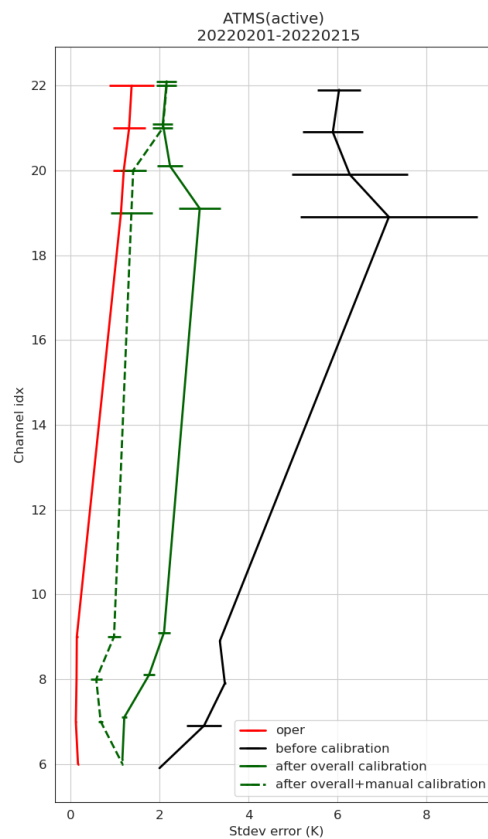


Figure 13: First guess departure statistics (standard deviation and absolute average difference) per channel in the “simulated world” before and after calibration and in the “real world” for ATMS active observations. Statistics covers 15 days.

First guess of EPS-Sterna observation errors was defined using 1) instrument specification document (NeDT, Table 2) and 2) existing instruments as proxy. Figure 14

illustrates the final values of observation errors for all instruments, after calibration, including those for EPS-Sterna.

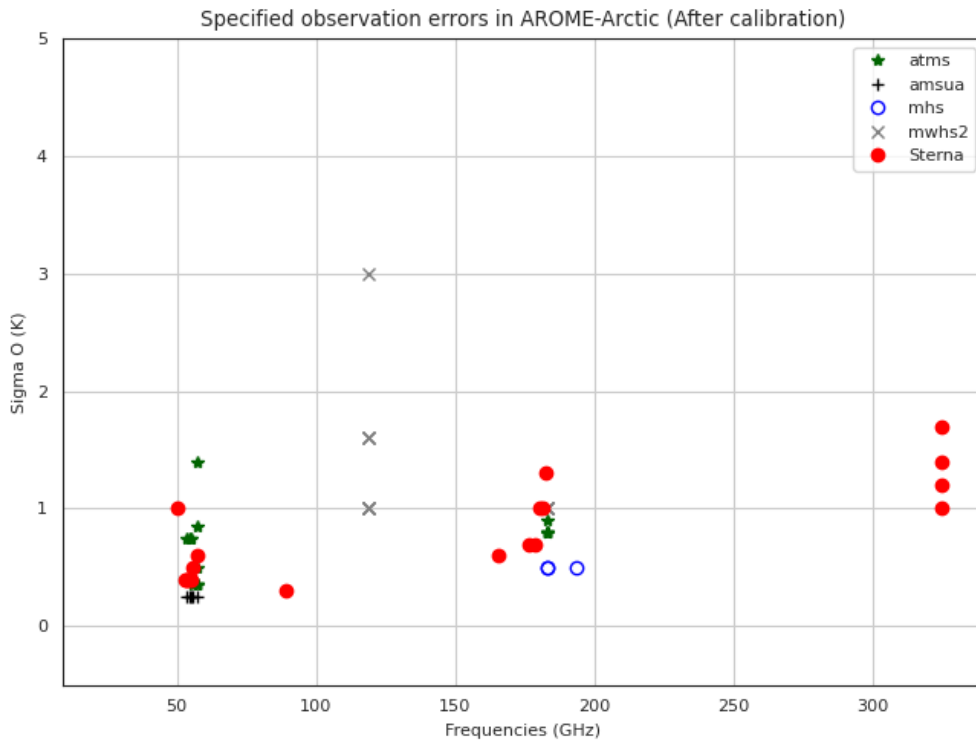


Figure 14: Specified observation errors in AROME-Arctic for microwave instruments, including a first guess for EPS-Sterna data (after calibration)

Channel		Obs error				
Name	Frequency			Sterna-31	165.5	0.6
Sterna-11	50.3	1		Sterna-32	176.311	0.7
Sterna-12	52.8	0.45		Sterna-33	178.811	0.7
Sterna-13	53.246	0.45		Sterna-34	180.311	1.2
Sterna-14	53.596	0.45		Sterna-35	181.511	1.2
Sterna-15	54.4	0.45		Sterna-36	182.311	1.3
Sterna-16	54.94	0.45		Sterna-41	325.15±1.2	1.7
Sterna-17	55.5	0.5		Sterna-42	325.15±2.4	1.4
Sterna-18	57.290344	0.6		Sterna-43	325.15±4.1	1.2
Sterna-21	89	0.3		Sterna-44	325.15±6.6	1

Table 6: Specified first-guess observation errors specified in AROME-Arctic for the perturbation and assimilation of EPS-Sterna data (after calibration).

#### 4.8 Simulation of EPS-Sterna observations, preprocessing and DA configurations

As detailed in section 3, a set of observation scenarios for various EPS-Sterna satellite constellations were provided to us by EUMETSAT for investigation. For these we simulated and investigated the impact of the provided six-satellites, four-satellites and three-satellites EPS-Sterna scenarios (denoted OP6-3SAT, OP2-4SAT, OP3-6SAT).

EPS-Sterna observations have been simulated in the same way as the existing observations (see section 4.3). We applied the following channel usage/blacklist setup:

- Fields of view located at the edge of the swath were rejected to restrain the assimilation to observations at +/- 45 degrees  
=> FOV positions within 15 and 100
- Window channels are rejected over all surfaces  
=> channel 1, 2, 9, 10
- 325 GHz group of channels are rejected over all surfaces (no expertise with these frequencies)  
=> channel 16, 17, 18, 19
- Surface-sensitive sounding channels are assimilated over sea-surfaces  
=> channel 3, 4, 5 as well as 11, 12, 13
- High-peaking sounding channels are assimilated over all surfaces  
=> channel 6, 7, 8 as well as 14 and 15

The blacklist and the thinning procedure has been set-up consistently to AMSU-A, MWHS-2 and MHS. For each assimilation window, all available observations provided by the same sensor (eg. eventually from several platforms) are mapped and thinned to 80 km. With regards to these operational sounders that are disseminated at high resolution, EPS-Sterna has been provided with a sampling distance of about 100 km. An example of the thinning procedure for EPS-Sterna Channel 5 at 6 UTC is presented in *Figures 15* and *16*. For this assimilation window, the data from 4 platforms are available (in the OP3-6SAT EPS-Sterna configuration). Two passes of each EPS-Sterna platform are available over the domain at that time (*Figure 15*). During the thinning procedure, EPS-Sterna observations from all platforms are mapped on the same grid, thinned at 80 km distance and quality checked. *Figure 16* shows a homogeneous map of resulting active EPS-Sterna observations over the AROME-Arctic domain.

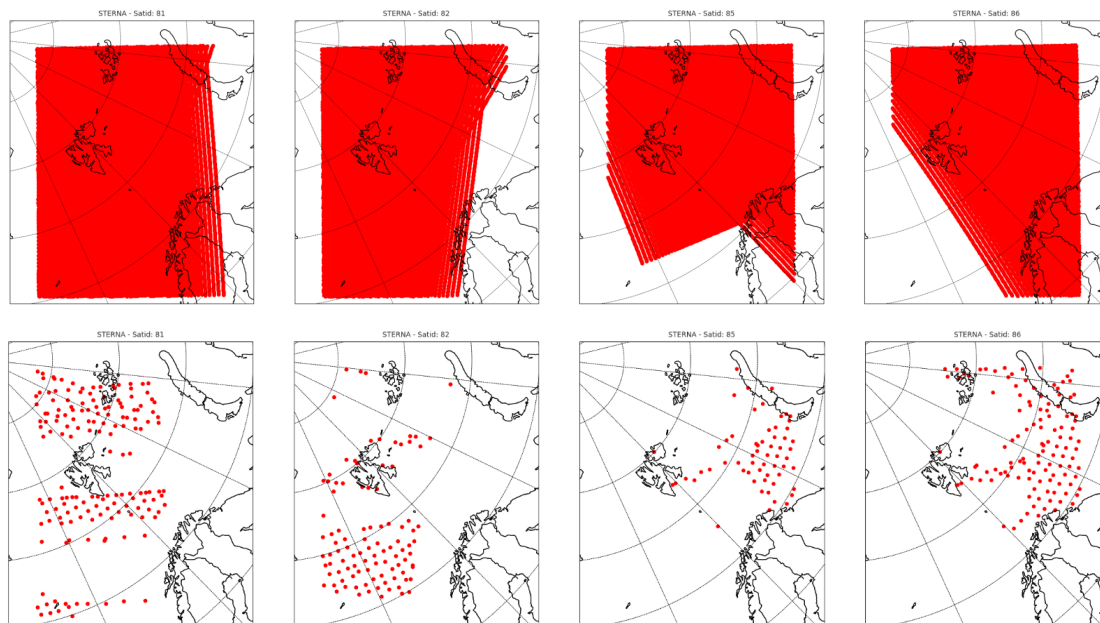


Figure 15: Example of available passes and thinking procedure of EPS-Sterna constellation at 06 UTC. Upper panel: Available observations. Lower panel: Assimilated observations from each of the passes.

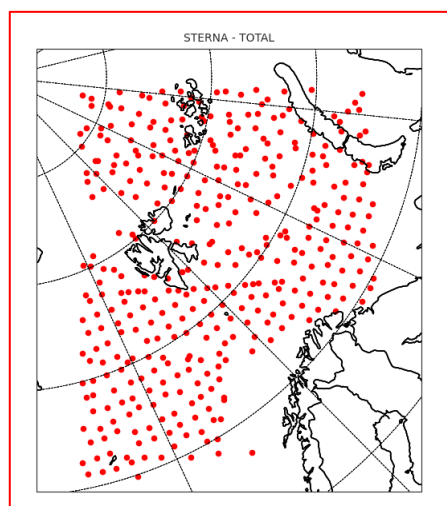


Figure 16: The total observation coverage for assimilation based on all the passes shown in Figure 15.

The OSSE has been used to assess four observation scenarios:

- **A control run:** Scenario assimilating satellite observations from AMSU-A, MHS, ATMS, MWHS-2 and IASI, in addition to radiosondes, aircraft and synoptic observations.

- **The EXP OP3-6SAT run:** Experiment scenario with all observations in the control run with addition of the 6 EPS-Sterna satellites over 3 orbital planes.
- **The EXP OP2-4SAT run:** Experiment scenario with all observations in the control run with addition of the 4 EPS-Sterna satellites over 4 orbital planes.
- **The EXP OP3-3SAT run:** Experiment scenario with all observations in the control run with addition of the 3 EPS-Sterna satellites over 3 orbital planes.

We can then assess the impact of the 3 constellations by considering the improvement in fit of the analysis and the forecast to the Nature Run versus that of the control run.

We should note that both the control run and the “EXP” runs use the same upper-air assimilation system with the same fixed background error covariance matrix. This matrix is estimated in our system using the recent, existing observing system. When increasing the amount of observations in the future, the covariances should ideally be recalibrated to obtain the optimal impact of the new observing system. Thus the assimilation is probably better adapted to the configuration in the control run than the “EXP” runs. This leads to some underestimation of the possible impact of EPS-Sterna observations in the experiments relative to optimally tuned systems.

The OSSE experiments are quite computationally demanding, so in these simulations we have run first on a 20-day period from 1 to 20 Feb 2022. The 3 first days of the runs was a spin-up phase, where we did not use the output. The period has been extended and the actual results presented here are for the period from 3 February to 27 February.

# 5. Results

## 5.1 Monitoring of active observations and complementarities

With the simulated observing scenarios outlined above, we can visualise the coverage of active EPS-Sterna platforms within our domain at the various times of the day in the different constellation scenarios. *Figure 17* and *Table 6* show 5-days-accumulated EPS-Sterna active observations per assimilation window and per platform for the 3 configurations (OP3-6SAT, OP2-4SAT and OP3-3SAT). The same result is presented for MHS active data as reference. Overall, due to the thinning strategy remapping all platforms together for each assimilation window, the total amount of active observations over 5 days is about 188 000 in OP3-6SAT, 176 000 in OP2-4SAT and 167 000 in OP3-3SAT and does not vary significantly. There is a compensation mechanism at play. It seems that more observations are used per single satellite in the OP3-3SAT scenario with regards to the OP3-6SAT scenario.

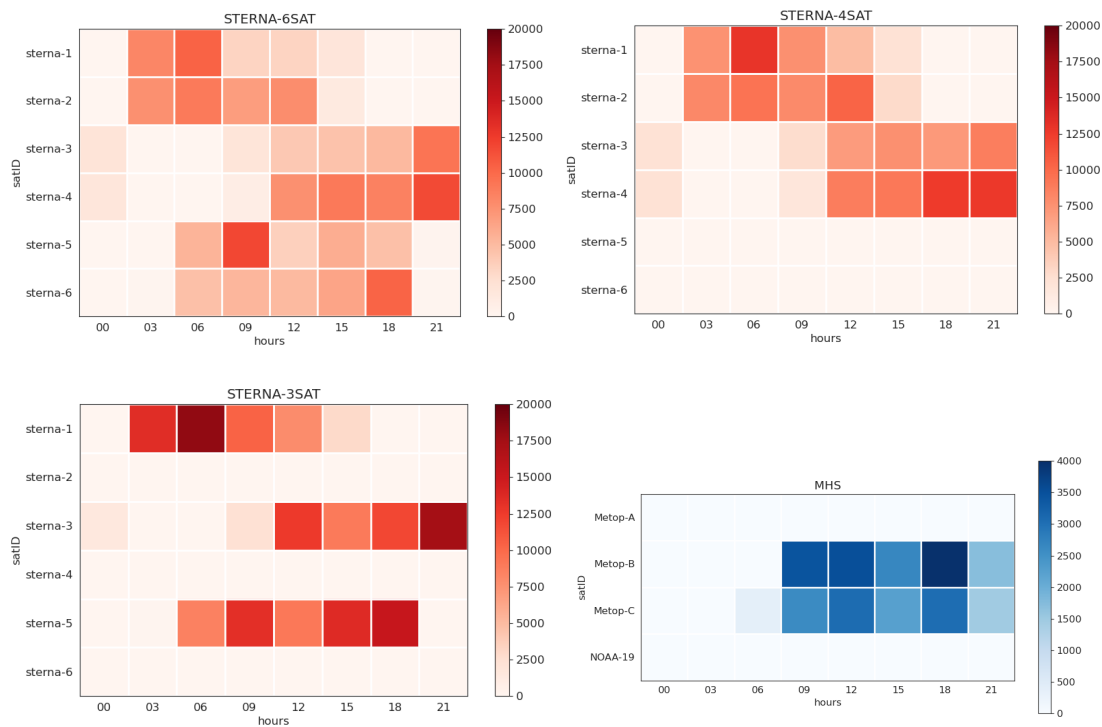


*Figure 17: 5 days-accumulated EPS-Sterna active observations per assimilation window and per platform for the 3 configurations (OP3-6SAT, OP2-4SAT and OP3-3SAT). The same result is presented for MHS active data as reference. The colour basis indicates the number of available observations after thinning.*

(UTC)	0	3	6	9	12	15	18	21
<b>OP3-6SAT</b>	2339	16071	29337	30066	31430	28812	28571	21346
<b>OP3-3SAT</b>	1514	13565	26802	25979	29513	25483	27049	17434
Ratio	0.64	0.84	0.91	0.86	0.93	0.88	0.94	0.81

*Table 7: Sum of active EPS-Sterna observations, all platforms accumulated over 5 days, per assimilation window and ratio between the 2 configurations (OP3-6SAT and OP3-3SAT). Synoptic situations and criteria might differ.*

In the following, we can see to what extent EPS-Sterna fills in gaps in the passive microwave observing system in our domain. In *Figures 18* and *19* we look at the coverage at 06 and 09 UTC, which were times where the coverage was not optimal and dense, respectively. We see that EPS-Sterna will give several passes within the time window for assimilation around 06 UTC, which will be relevant for filling in the coverage at this time, where AMSU-A and MHS are missing. By analysing 09 UTC, we want to see if the system is able to add more EPS-Sterna observations on top of a dense observing system. It shows a good ability to fill in with information at this time. This EPS-Sterna configuration was designed to fill in well with the other sounder's orbit configuration, so this demonstrates that an EPS-Sterna constellation expectedly provides complementarity to other microwave sounders available.

In addition, it is important to mention that the data assimilation system compensates the lack of MW soundings in OP3-3SAT by assimilating more soundings from other satellites. This, however, does not bring an equivalent impact of the OP3-6SATs scenario. So even if there is compensation in the system, the two scenarios are not equivalent from an impact point of view.

Maps of active MW observations  
(2022021206)

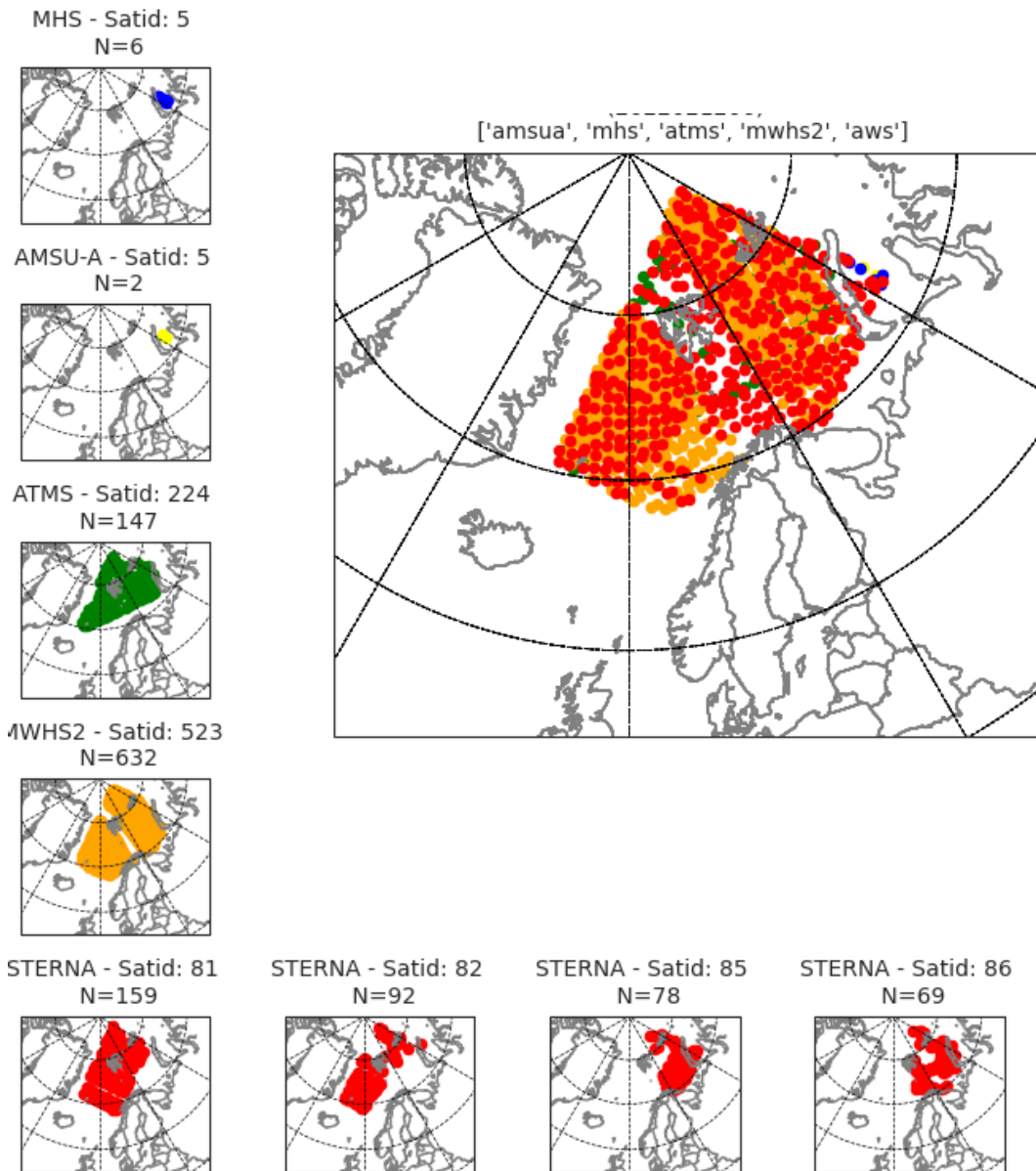


Figure 18: Map of active observations from microwave sensors and EPS-Sterna (OP3-6SAT) on the 12/02 at 06 UTC

Maps of active MW observations  
(2022021109)

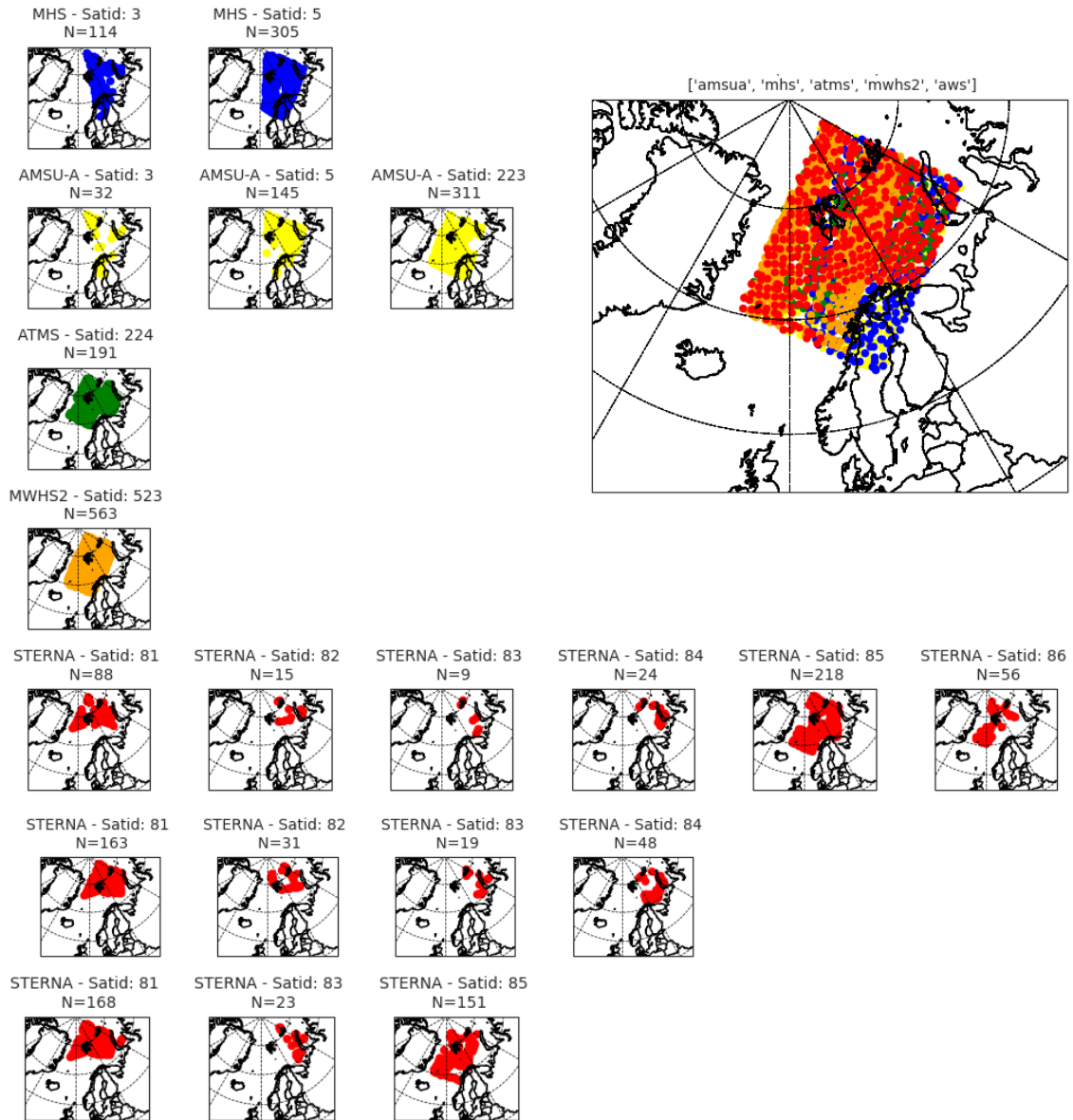
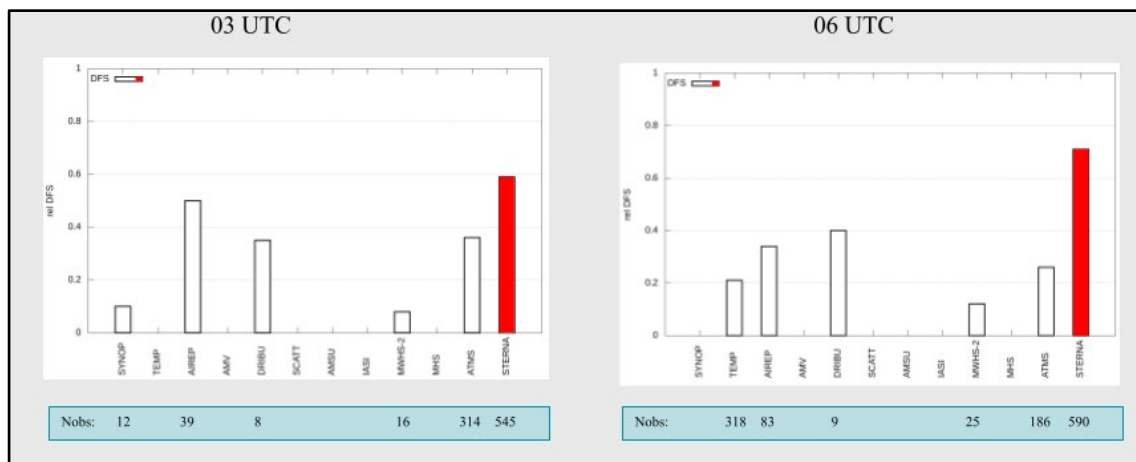


Figure 19: Map of active observations from microwave sensors and EPS-Sterna (upper line: OP3-6SAT, middle: OP2-4SAT and lower line: OP3-3SAT) on the 11/02 at 09 UTC.

## 5.2 Impact on the analysis

The aim of this section is to evaluate how the system is able to process and ingest the information provided by the 3 different configurations (OP3-6SAT, OP2-4SAT and OP3-3SAT). As it was shown in the previous subsection, the geographic coverage, and the amount of active data from each configuration, can change quite significantly between assimilation windows. The interaction with other observing systems will also play a significant role in finding the new balance to produce the optimal atmospheric analysis.

First, we have assessed the impact of the different observation types by calculating their Degrees of Freedom for Signal (DFS) (Rabier et al, 2002, Fisher, 2003, Chapnik et al, 2005). DFS is a measure from information theory, in this case, of how much each observation type affects the analysis, taking into account the extent to which they provide independent information and fill gaps and not overlap with other observations. Our analysis, not unexpectedly, shows that the DFS contribution of EPS-Sterna varies with the time of day, depending on the amount of other observations available. In *Figure 20* and *21*, we find a very high, if not dominating impact at 03 and 06 UTC, particularly taking into account the large number of EPS-Sterna observations. For 09 and 15 UTC the DFS impact per EPS-Sterna observation is smaller, reflecting more presence of other, overlapping observations at these times.



*Figure 20: Relative impact expressed as degrees of freedom for signal (DFS) per observation of EPS-Sterna at 03 (left panel) and 06 (right panel) UTC over AROME-Arctic domain. The numbers below show the total number of observations for each observation type.*

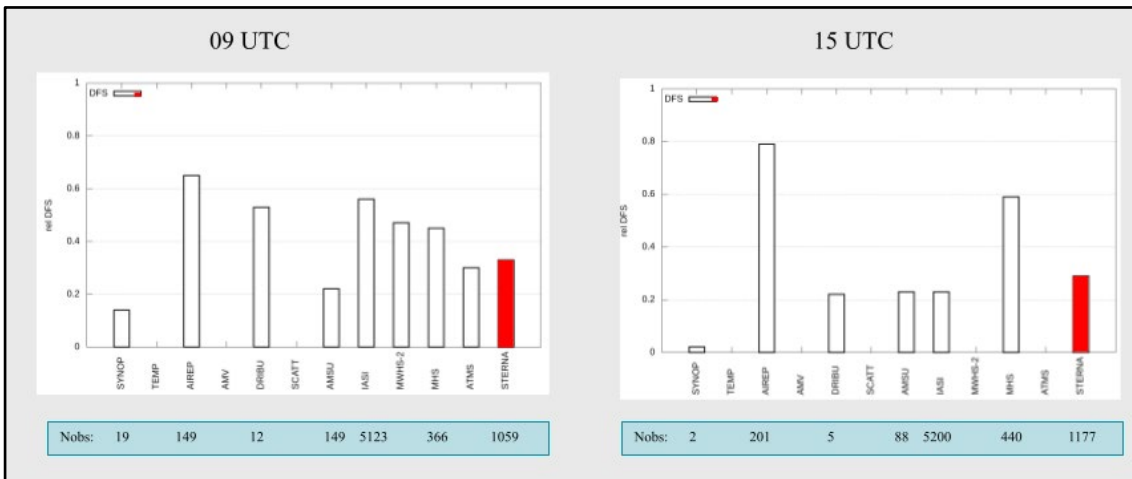


Figure 21: As for Figure 20, but for times 09 and 15 UTC.

DFS could also be very informative if the relative DFS value is translated in a total percentage contribution for all observations (Figure 22), also as a function of time over the day for TEMP and MW (Figure 23), over the domain.

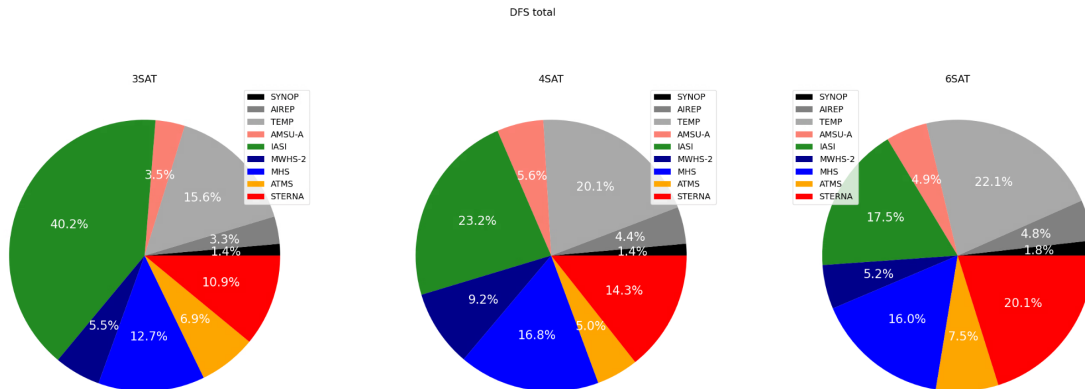


Figure 22: Total percentage contribution of each observation type in the atmospheric analysis over 7 days (20-27/02)

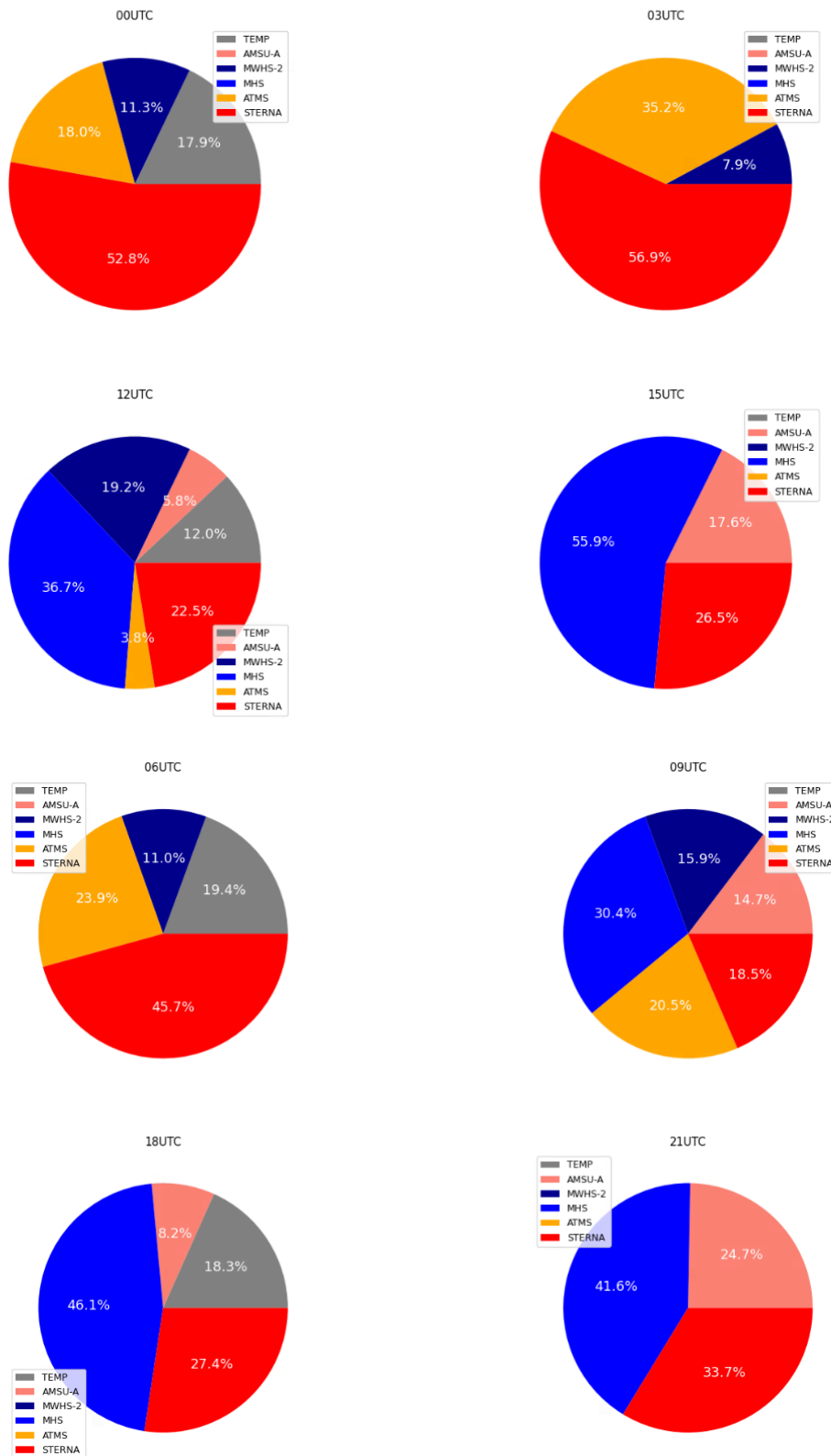


Figure 23: Total percentage contribution of microwave observation types and radiosondes (TEMP as reference) in each 3h-atmospheric analysis averaged over 7 days (20-27/02)

To go further into the OSSE impact results, we show statistics on how the assimilation of the EPS-Sterna constellation affects the analysis, as verified by comparisons with the Nature Run. By nature, assimilation generally creates increments to draw the model state in an average sense towards the truth, i.e., the Nature Run in this case (or observations plus associated uncertainty from the Nature Run sampling). The final assimilation increments resulting from the assimilation of the observations are also determined by the fixed background error covariance matrix of the assimilation scheme. This matrix implicitly provides structure functions describing how errors at a certain point correlate with errors in nearby points and how an error in a particular physical quantity correlates with errors in the other physical variables. Thus, for instance, an adjustment in temperature through a temperature observation will also provide an adjustment in the wind field, through the structure functions. These covariance structures have been determined statistically as overall average structures (for AROME-Arctic by downscaling of an ECMWF ensemble serving as a proxy providing probable properties of forecast errors). They do not provide a perfect representation of the error structures on a case-to-case basis.

In *Figure 24* and *25* we show the impact statistics of the EPS-Sterna constellation on the analysis. We note that, as expected, the assimilation of EPS-Sterna improves the fit to the Nature Run truth. For temperature, the improvements are seen mainly in the mid-troposphere, and near the surface the average improvements vanishes. This is related to the fact that the surface-sensitive channels of EPS-Sterna have been left out in the experiment as described above. It may also have a contributing explanation in the use of unperturbed boundary conditions coming from the Nature Run. Thus, the potential increments near-surface would come from the structure functions extrapolating information statistically from EPS-Sterna information higher up. There is ongoing work on available methods for handling the surface emission in the assimilation scheme which would have improved the situation (being done in the ESA-AWS project mentioned above), but these developments were not ready for implementation in our OSSE system here. Thus, the lack of improvements in the analysis near the surface is not realistic for what we would expect in a real assimilation system.

For the specific humidity verification, we see improvements all throughout the atmosphere. The improvements are highest near to the surface, which shows that the extrapolation through the structure functions here works better than for temperature. It also reflects the fact that typical specific humidity values are largest near the surface and generally decrease exponentially-like with height.

For the wind verification, we also note here that we see qualitative improvements in the mid- and lower troposphere. Since the EPS-Sterna observations have no direct dependence on the wind, these increments come purely from the correlations implicit in the structure functions, which here seem to work well. The fact that a larger improvement can be seen in the zonal than in the meridional component of the wind, is probably related to the orbit geometry: The likely explanation is that there is more likelihood to sample

strong north-south temperature variations rather than longitudinal variations, and this is reflected in the structure functions.

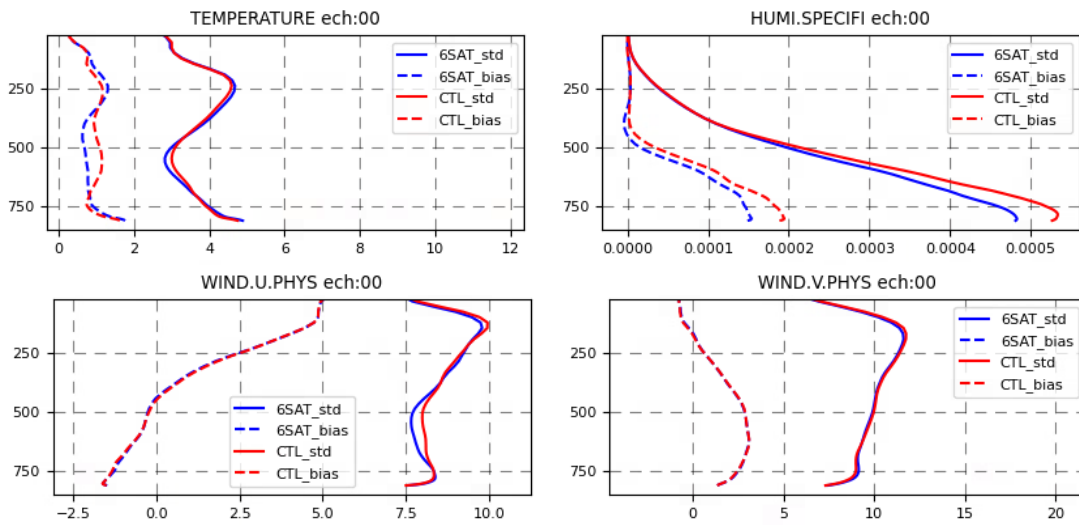


Figure 24: Impact of the OP3-6SAT EPS-Sterna constellation. The curves show bias (dotted lines) and standard deviation (solid lines) of the departures from the Nature Run. Red curve: The control run without EPS-Sterna. Blue curves: The run with OP3-6SAT EPS-Sterna constellation added on top of the observing system of the control run. The panels (from left to right) are for temperature, specific humidity, zonal and meridional components of wind, respectively.

In the time series plot of the verification statistics in Figure 25, we see that the improvements are not evenly distributed in time. There is some tendency that we see the largest improvements in the forecasts when the actual errors in the forecast are the largest.

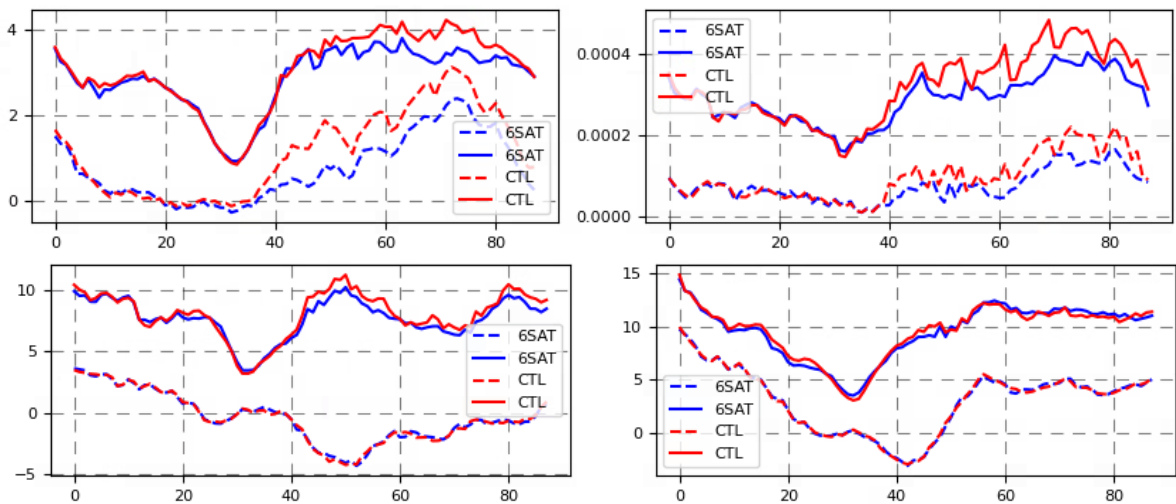


Figure 25: Time series of the bias (dotted line) and standard deviation (plain line) of the departures from the Nature Run at 550 hPa, which is around where we see the maximum impact, for the same quantities as in Figure 24. X axis corresponds to cycles index. The first 40 cycles (5 days) may be affected with spin-up issues.

### 5.3 Impact on the forecast

In this section, the forecast impact of the OP3-6SAT, OP2-4SAT and OP3-3SAT EPS-Sterna constellations are evaluated. The model has been run with these three configurations up to 24h forecast length as previously discussed in Section 4.

Figure 26 shows the overall impact of the OP3-6SAT, OP2-4SAT and OP3-3SAT EPS-Sterna constellation as compared to no-Sterna in terms of relative change (%) in forecast error (root-mean-square error) compared to the Nature Run. We see that the largest error reduction in terms of relative change in forecast error occurs in temperature, with around 10% reduction in forecast errors around 500 hPa for the short-range forecasts (up to 12h). We note that near the surface there is no improvement in temperature, rather a small degradation, reflecting what was mentioned in the previous section that the temperature analysis does not improve on the lower levels. This is due to the blacklisting of low-peaking channels, as previously mentioned in Section 4.5 and temperature increments at these levels are derived from structure functions only. As mentioned above, this is not a realistic result in a real assimilation system, which can handle and assimilate surface affected radiances.

For specific humidity, we see relative improvements in a deeper layer and all the way down to the surface. We also see improvements in the wind forecasts, up to around 5% improvement around 500 hPa for the short forecast ranges. It is also encouraging to see that the wind improvements seem to propagate down to the surface with time, with an improvement maximum in near-surface zonal winds around 12 hours forecast range. These results are consistent with Randriamampianina et al, 2021.

For all these physical quantities, we see a decay in the improvements towards the longer forecast ranges towards 24 hours. Here it should be noted that this is influenced by our use of “perfect boundaries” using the Nature Run to force the lateral boundaries. Section 5.4 is discussing the impact of the surface analysis on a shorter period. In fact, it was shown that when the surface data assimilation is not performed (i.e. the previous short range forecast is used), the impact of Sterna is smaller along the vertical but constantly beneficial.

Ideally, we should have performed the experiments with realistic inaccurate boundaries from a global model using the same observation scenarios as our experiments. In reality, there will also be an impact of use of EPS-Sterna also coming from the lateral boundaries which we cannot see here by design. We can expect that in a real regional system the impact of EPS-Sterna is expected to last longer, through the impact coming from the lateral boundaries. If we look at similar figures as these from the Météo-France companion study, we see that the time scale of the impact in their global system is much longer than what we see here.

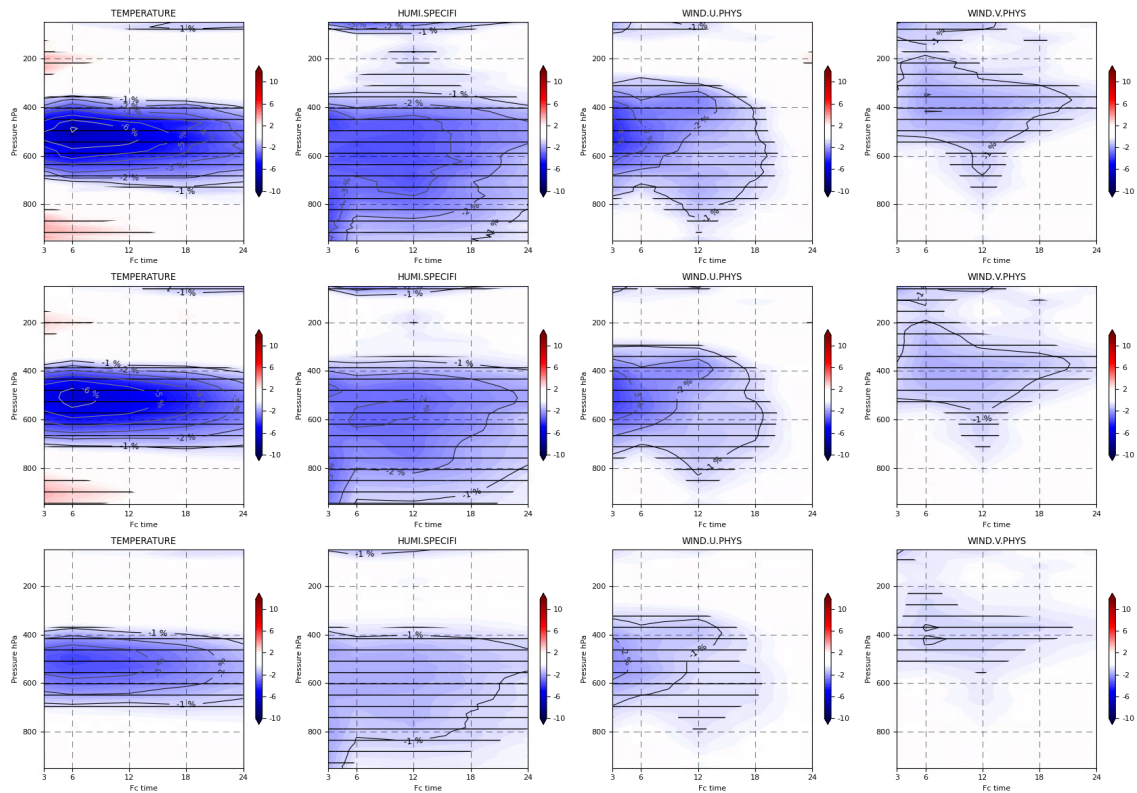


Figure 26: The figure shows the impact of OP3-6SAT (upper line), OP2-4SAT (middle line) and OP3-3SAT (lower line) over AROME-Arctic domain expressed in terms of relative change (%) in forecast error (root-mean-square error) compared to the Nature Run. Red shadings indicate degradation, blue indicate improvements. The black line areas indicate that the improvement is significant with 95% confidence level. From left to right, each panel shows results for temperature, specific humidity, zonal and wind components.

For all constellations we find similar structures and evolutions of the improvements. It only gets weaker in magnitude when reducing the number of satellites. In OP3-3SAT, the negative impact on the short-range forecast of temperature has been reduced. This negative impact could be the sign of a miscalibrated background error matrix, unable to spread additional information in temperature. It could, as well, be related to the surface treatment in the OSSE. As shown in Figure 27 from Randriamampianina et al, 2021, the assimilation of conventional observations in a regional forecast system can be detrimental on the vertical, especially around 250 hPa, creating wrong increments.

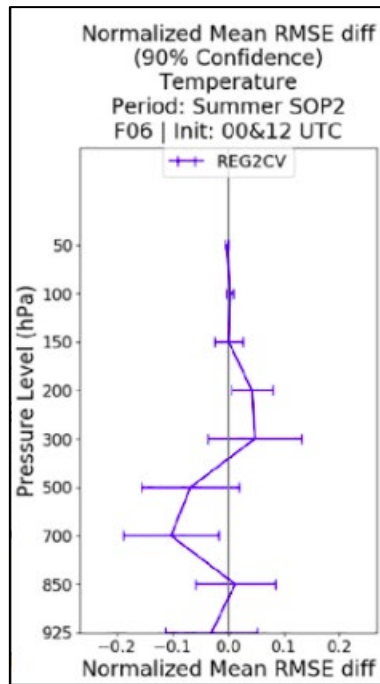


Figure 27: Difference in mean root-mean-square error (RMSE), normalised by the mean scores, of 6-hr forecast for temperature between one experiment in which all observations are used in LBC and one experiment in which conventional observations are denied from the regional DA. The impact of all conventional observations through regional DA is shown. Negative/positive values indicate positive/negative impact of observations on forecast skill. A 90% two-sided statistical significance test is applied, and verification is against the eight radiosonde stations in the AROME-Arctic domain (figure taken from Randriamampianina et al, 2021).

To track the evolution of the observation impact in the forecast, a sensitivity diagnostic called Moist Total Energy Norm (MTEN) is used. This diagnostic is a powerful technique based on the change in the energy norm between a reference and an experiment at a given forecast time. The concept of MTEN is described by Storto and Randriamampianina (2010). This diagnostic is highly situation-dependent and might be subject to large variations on a case-by-case basis. In this present study, the reference is the assimilation run without EPS-Sterna data and the results are taking into account surface pressure, temperature, specific humidity and wind speed over the 65 levels of AROME-Arctic. Figure 28 shows the overall relative change (in %) in MTEN at 00 UTC and 12 UTC for each constellation scenario of EPS-Sterna. As expected, the impact of all constellations is stronger at 00 UTC when the atmospheric analysis is not constrained with many other microwave instruments. It can be noted also that the impact is significantly reduced after 18h forecast length when the influence of the lateral boundary conditions is getting more dominant. Here, in the future conditions, it is expected that EPS-Sterna which will be also assimilated in the global system will indirectly benefit to the long-range forecast of AROME-Arctic. Comparing OP2-4SAT with OP3-6SAT, it can be seen that the added value by OP3-6SAT is larger at 00 UTC than at 12 UTC, indicating a possible saturation effect at 12 UTC when more other microwave sounders are available.

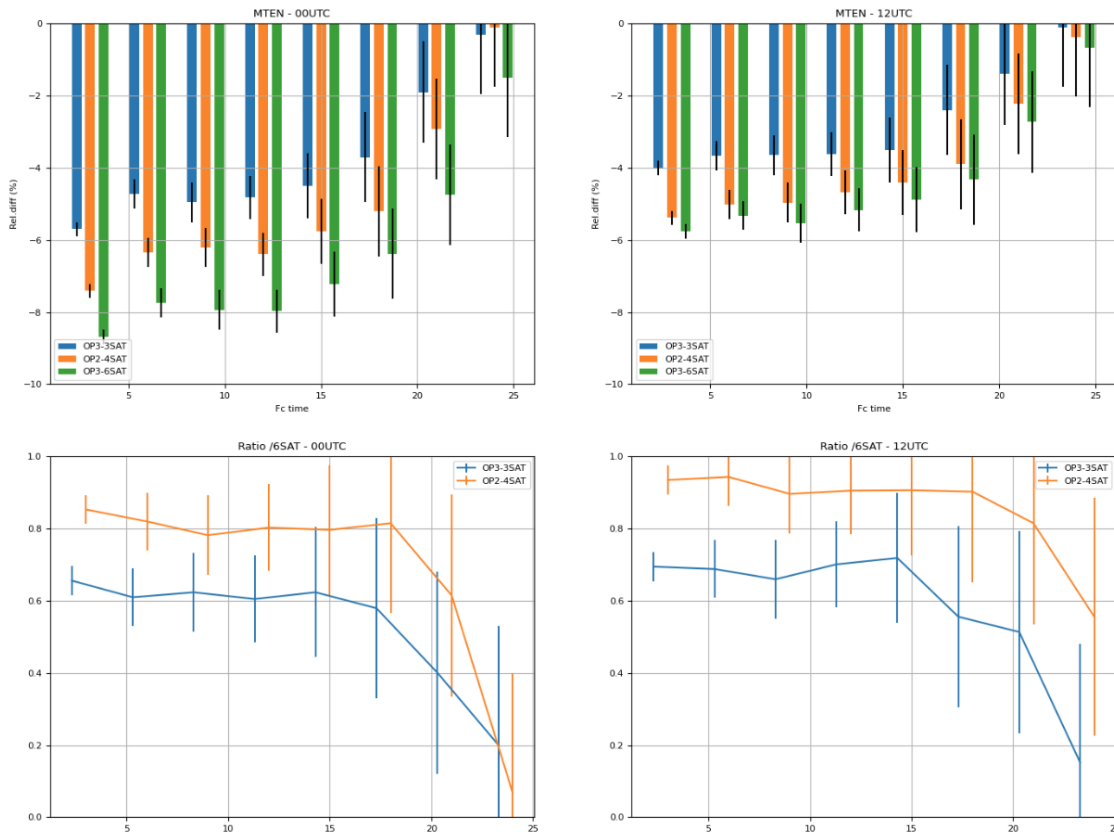


Figure 28: Relative difference (in %) of MTEN at 00 UTC and 12 UTC for the 3 constellation scenarios compared to the CTL where no EPS-Sterna have been assimilated (upper line). X axis is time in hours. The ratio between the 2 degraded scenarios and OP3-6SAT is also presented (lower line). The diagnostic has been run for the period from 20 to 27th of February 2023.

#### 5.4 Additional “short” experiments and case study

To complement the evaluation of EPS-Sterna impacts in the Northern latitudes, we have run 2 additional experiments (on a shorter period due to resource availability) and focus on the 15th of February as a case study.

##### Denial of Metop-B sounding sensors

Within the AROME-Arctic system, a set of instruments from Metop-B are assimilated. In fact, except ASCAT, which is assimilated in the operational version of AROME-Arctic, AMSU-A, MHS and IASI are assimilated in the control experiment of the OSSE. From the Météo-France and ECMWF companion studies performed at global scale, it was shown that the impact of EPS-Sterna would be equivalent to one Metop platform (which also includes AVHRR, a radio occultation sensor, GRAS, and the optical spectrometer GOME-2). Figure 29, 30 and 31 show the relative change in the standard deviation for the analysis and 3h-forecast and 24h-forecast of specific humidity for 3 configurations (OP3-6SAT, OP3-3SAT and No Metop-B) relative to the CTL.

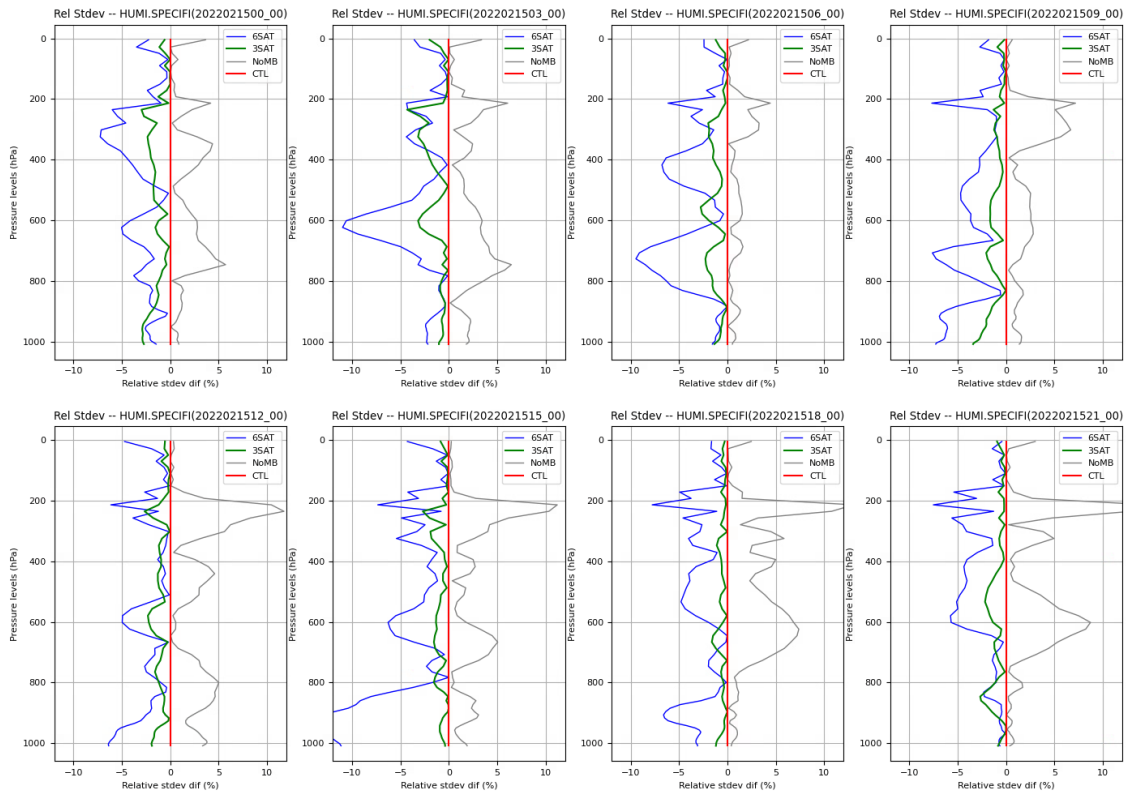


Figure 29: Relative difference in the standard deviation (in %) of analysed specific humidity versus the Nature Run at each assimilation time (00, 03, 06, 12, 15, 18 and 21 UTC) for the OP3-6SAT in blue and OP3-3SAT in green constellation scenario and the No Metop-B experiment in grey compared to the CTL in red. No EPS-Sterna have been assimilated in the denial nor the control run. Negative/positive values indicate positive/negative impact of observations on forecast skill. The statistics have been run for the 15th of February 2023.

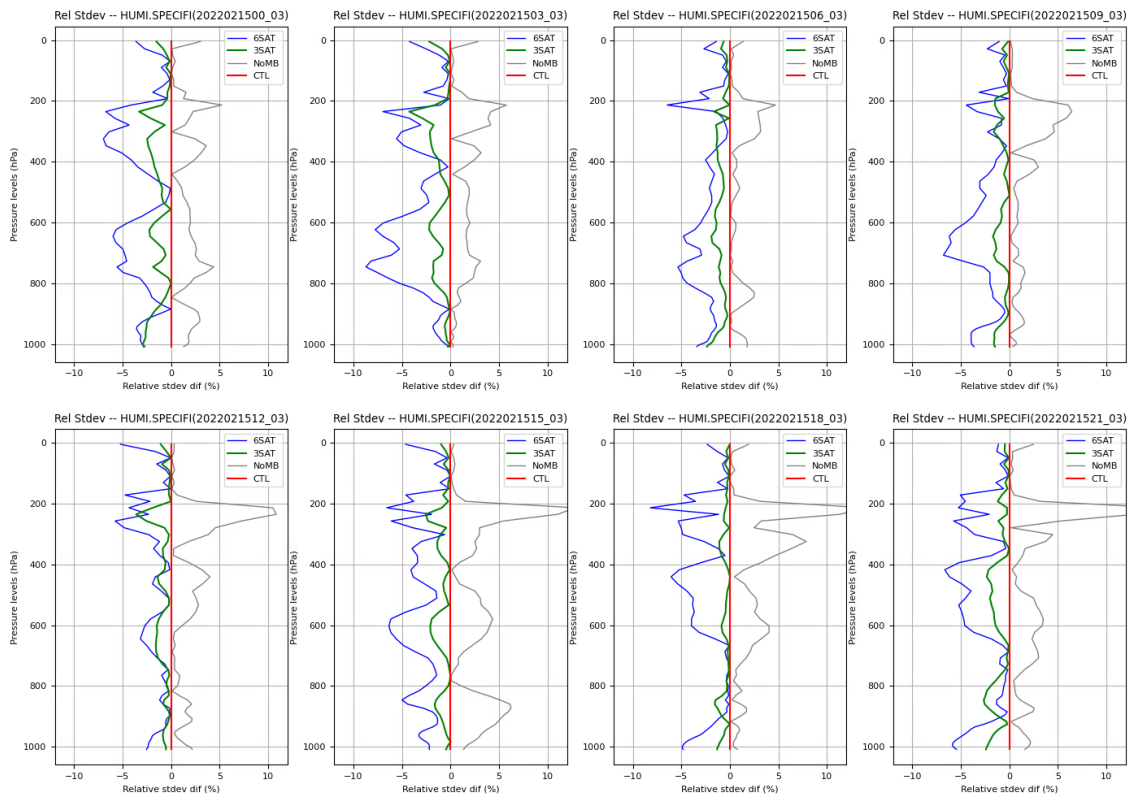


Figure 30: Same as 29 but for the 3h-forecast.

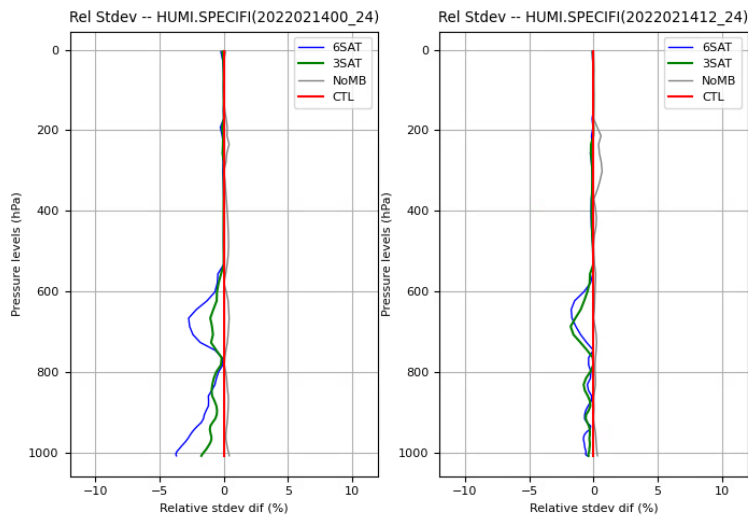


Figure 31: Same as 29 but for the 24 h-forecast and based on 00 and 12UTC analysis (valid at the analysis of 15th of February).

Overall, within the framework of this OSSE and over this period of time, the loss of Metop-B would induce a degradation of the specific humidity analysis of about 1.97% whereas the assimilation of EPS-Sterna improve on average the analysis of about 3.22, 1.54 and 1.04% respectively for OP3-6SAT, OP2-4SAT and OP3-3SAT.

On the 12h-forecast, EPS-Sterna reduced the relative standard deviation error of about 2.56%, 1.45% and 0.86% whereas the loss of Metop-B would degrade the forecast of 1.7%.

In average on the temperature, the loss of Metop-B would degrade the 12h-forecast of about 1.03% in term of temperature whereas EPS-Sterna would generate an improvement of about 1.9%, 0.92% and 0.83% respectively for OP3-6SAT, OP2-4SAT and OP3-3SAT. On the analysis, the loss of Metop-B would be of about 0.79% and the improvement related to EPS-Sterna would be of about 2.41%, 1% and 0.93% respectively for the 3 configurations.

### No surface assimilation

In the previous section, a slight degradation of the near-surface temperature forecast scores was noticed with the assimilation of OP3-6SAT and OP2-4SAT constellation of EPS-Sterna. This impact was found to be similar to the one that conventional observations could have in the regional system (following *Randriamampianina et al, 2021*). Some interactions between the assimilation of EPS-Sterna and the surface could partly explain this feature. In order to go further into details with this finding, we have performed a short data assimilation experiment in which the surface assimilation component has been deactivated. Instead of assimilating perfect/unperturbed surface observations and generating an atmospheric forecast “coupled” with a surface analysis (as it is set in operations), we have combined the atmospheric analysis and surface first guess together as initial conditions to the atmospheric forecast. *Figure 32* shows the change in the standard deviation (in %) of the OP3-6SAT configuration with (in black) and without (in blue) the surface analysis compared to the Nature Run, in relatively to the CTL configuration. When the surface analysis is deactivated, the impact of Sterna is smaller but constantly beneficial, also near-surface, on this period.

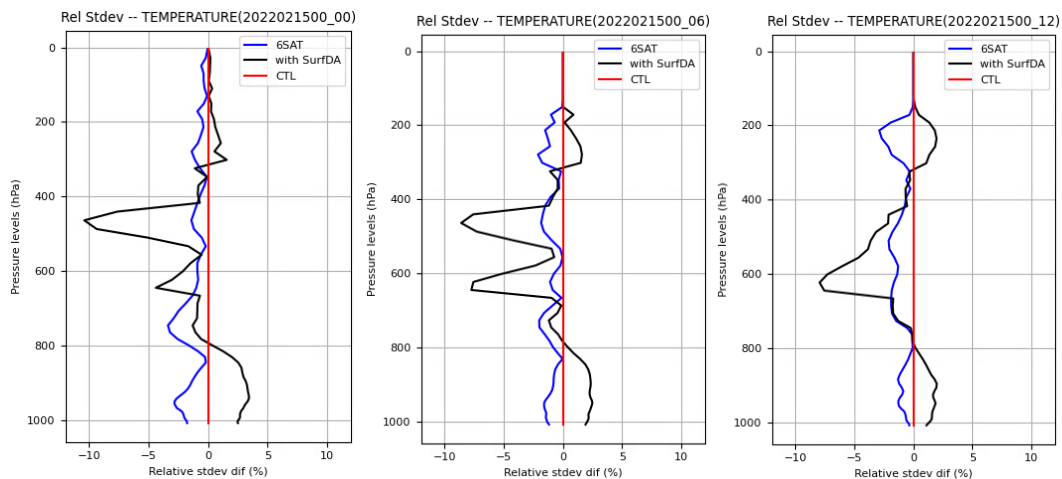


*Figure 32: Relative difference in the standard deviation (in %) of analysis (left panel), 6h-forecast (middle panel) and 12h-forecast (right panel) of temperature versus the Nature Run. Forecast is based on the analysis of 00 UTC.*

## Case Study: Precipitation events

Precipitation forecast is a key parameter in the Northern latitudes to prevent damages due to large amounts of snow in winter. Figure 33 shows maps of 5-day accumulated precipitations over the domain in February 2022. The cumulation takes into account the rain, the snow and graupel. With regards to the CTL run in which no EPS-Sterna were assimilated, both OP3-6SAT and OP2-4SAT seem to produce a larger amount of precipitation in the South west of Svalbard which is more consistent with the Nature Run (i.e red circle). In particular, the maximum in OP3-6SAT seems slightly shifted toward the south. This might indicate that OP3-6SAT is producing a better forecast of precipitation both in terms of location and quantity the OP2-4SAT and OP3-3SAT as well (not shown).

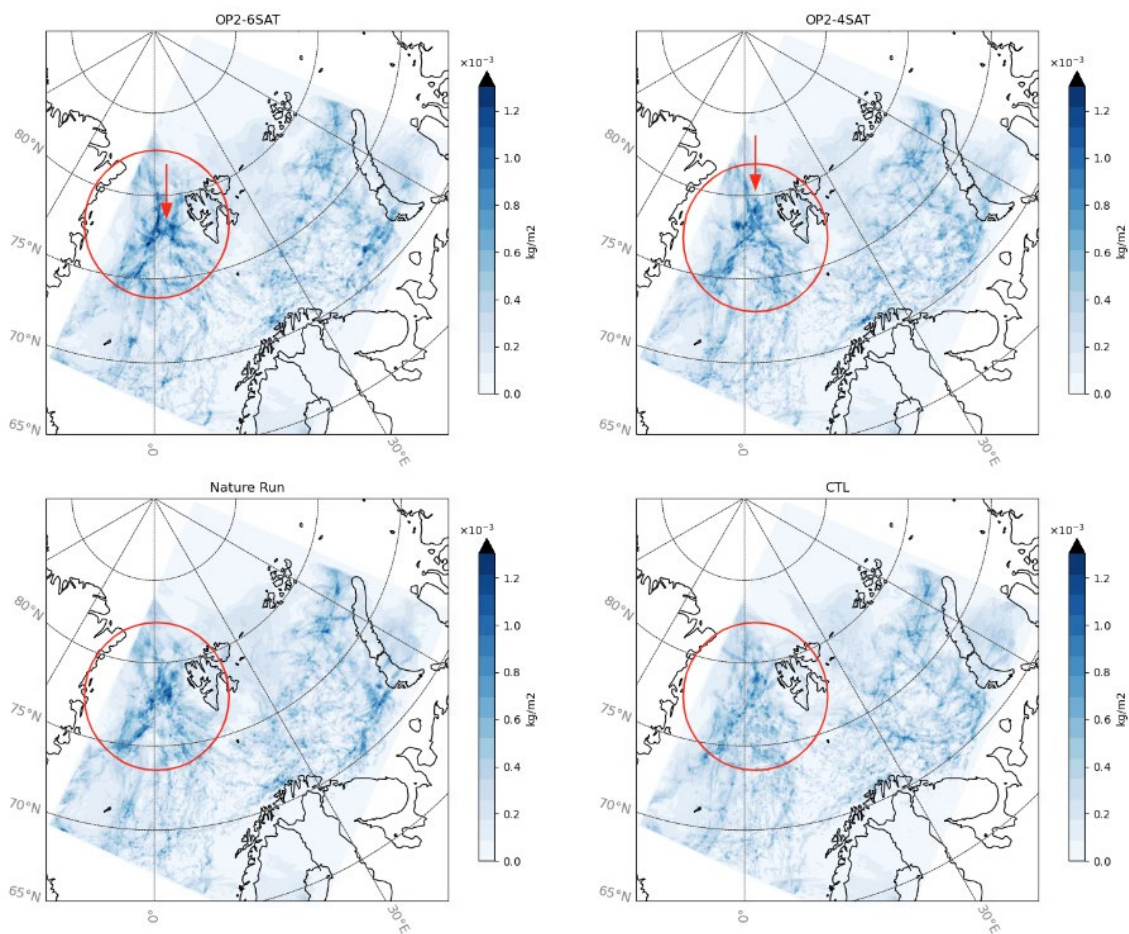
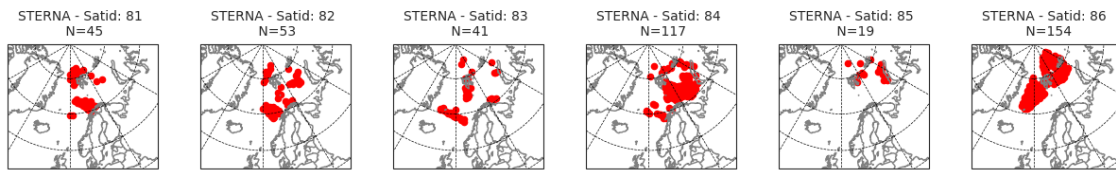


Figure 33: 5-days accumulated precipitation (rain+snow+graupel) over the AROME-Arctic domain as analysed in the experiments with EPS-Sterna OP3-6SAT and OP2-4SAT, in the CTL (without EPS-Sterna) and in the Nature Run. Data covers the period from 10 to 15th of February 2022.

Regarding the forecast impact, we focused on one case in particular, where a large amount of EPS-Sterna observations were assimilated on top of those provided by other MW platforms. Figure 34 shows the maps of active EPS-Sterna observations in OP3-6SAT on the analysis time of 15/02/2022 at 12UTC. These observations have been assimilated in

the analysis that produces the 12h-forecast presented in *Figure 35*. Again, with regards to the CTL experiment in which no EPS-Sterna is used, the distribution of the precipitations cells seems better located in OP3-6SAT compared to the Nature Run field.



*Figure 34: Maps of active EPS-Sterna observations in OP3-6SAT configuration on the 15/02 at 12UTC.*

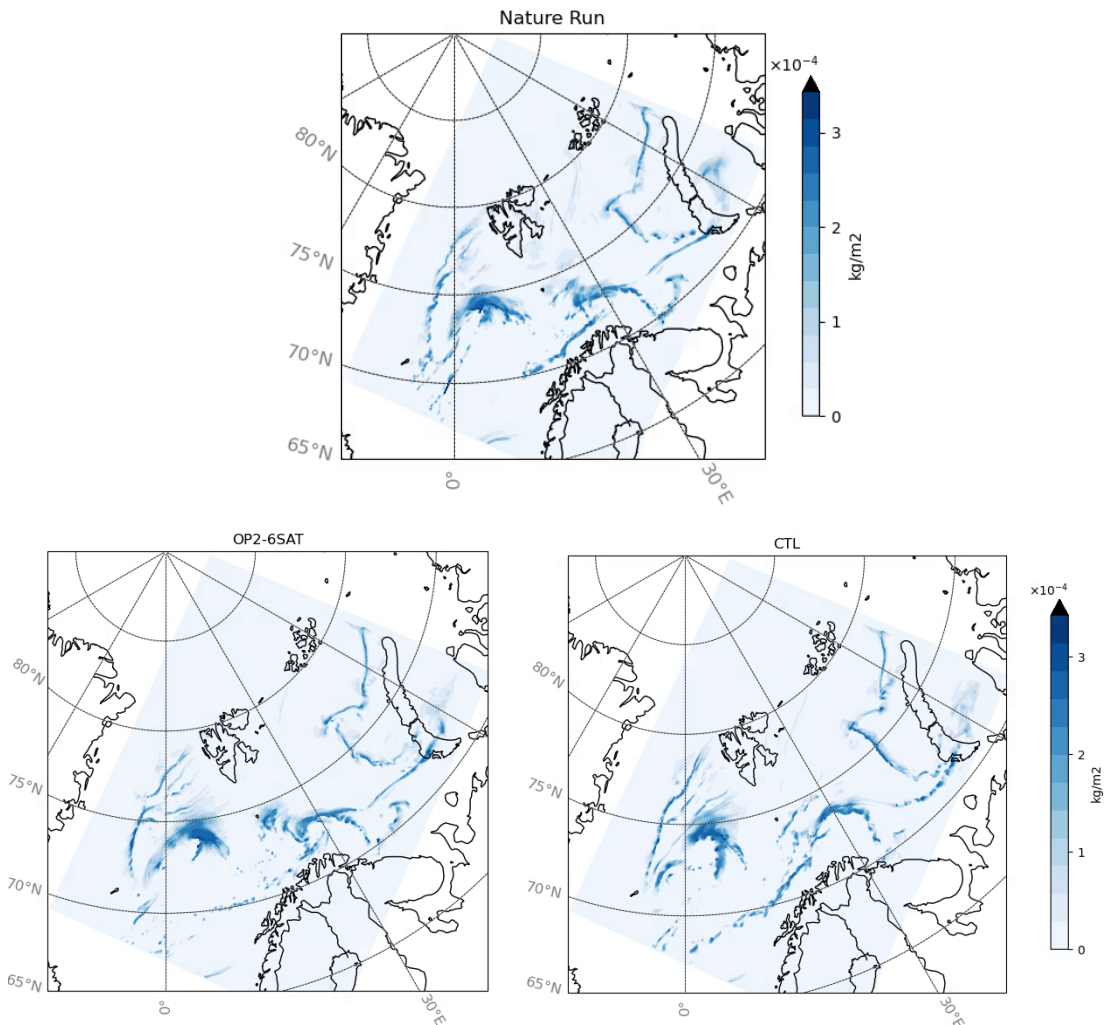


*Figure 35: Maps of precipitation as produced in the Nature Run on the 16/02 at 00UTC compared to 12h-forecast valid on the 16/02-00h based on the analysis of the 15/02 at 12UTC from the OP3-6SAT configuration and the CTL.*

## 6. Discussion

We have performed an OSSE experiment to assess the impact of EPS-Sterna on top of the existing observing system in the context of the forecasts from our AROME-Arctic NWP system. We generally see that the EPS-Sterna constellation is likely to complement the existing observing system well, providing good overall improvements of forecast scores versus the control run. The overall impact of EPS-Sterna was especially strong in the early morning. For short forecast ranges (from 3 to 12h) we see pronounced improvements in wind and temperature in the mid troposphere. For the OP3-6SAT scenario the average relative error reduction for temperature is around 3 to 4% on average, reaching 7% for analysis and short-range forecasts in mid-troposphere. This constellation also improves wind forecasts with ~5% for the short ranges. As a comparison, existing instruments used in the CARRA reanalysis system were shown to produce an error reduction of about 2% in temperature and humidity (Dahlgren, 2023). For the zonal wind the mid-troposphere improvements of EPS-Sterna propagate downwards with increasing forecast range. Looking at the time series of the analysis impact, we find that the relative improvements generally seem larger in situations with large forecast errors.

Additional “short experiments” explored the impact of EPS-Sterna compared to the sounding sensors (AMSU-A, MHS and IASI) of one Metop. It was shown that the impact of EPS-Sterna OP2-4SAT is about equivalent to that from Metop-B in this study. The OP3-6SAT shows a stronger impact, especially in the early morning. In these additional experiments, we also partly explained the degradation seen in the temperature forecast with the assimilation of EPS-Sterna. This feature was probably triggered by the surface analysis. Finally, a case study on precipitation was presented. Results from a qualitative “eyeball analysis” of the precipitation patterns indicated that the assimilation of EPS-Sterna would have some potential to improve the analysis and the forecast of snowfall spatially and quantitatively, although impacts in such case studies generally will vary from case to case. Results from these three additional short studies are on quite limited time periods which limits the robustness of these results.

A main limitation of this study is that improvements coming from EPS-Sterna assimilation through lateral boundaries from a host model are not taken into account. The setup uses “perfect” lateral boundaries from the Nature Run. This means that in a real regional NWP system the impact is expected to be significantly larger. With more realistic lateral boundaries as in real life, together with a refined background error matrix, we also expect the impact of EPS-Sterna to last longer in the system. The magnitude and duration of such additional improvements are still not known and could be a topic for future studies using the results from the parallel global NWP OSSE study.

It is also a limitation that we have not assimilated the surface sensitive EPS-Sterna channels, which we would have had capability to do in a more realistic operational system. This, together with not perturbing the surface observations as part of the OSSE, limits the total impact and in particular the impact on near-surface variables. Together with an adequate surface analysis (with perturbed observations), it would potentially have removed the negative impact we found on the low-level temperatures at short-range forecast.

Finally, considering that EPS-Sterna gives a very dense observation coverage and frequent revisit, use of the data in regional NWP systems with even more rapid refresh could be very interesting and have a potential for significant improvements in very short-range forecast products. The way the global NWP systems or the AROME-Arctic system are set up at present, there is likely an under-exploitation of EPS-Sterna information content both by spatial thinning and by lumping together all observations in three-hour intervals as done in AROME-Arctic. Exploitation of EPS-Sterna in a system like MetCoOp Nowcast could yield a good impact, and it is likely that future systems will evolve with even higher horizontal resolution and assimilation systems better adapted to dense and frequent observations, which would benefit even more from an EPS-Sterna constellation.

## Acknowledgements

This study is funded by EUMETSAT under frame contract EUM/CO/22/4600002671/CJA, and the work has benefited from discussions with Christophe Accadia at EUMETSAT. We are grateful to colleagues at Météo-France for their kind provision of the ARPEGE Nature Run used for this study.

## List of Tables and Figures

*Table 1: Operational models used in forecasting at MET Norway (and other Scandinavian countries)*

*Table 2: Sterna channel list and characteristics applicable this study of EPS-Sterna*

*Table 3: Orbital plane and satellite number associated to shifted starting time (Walker constellation criteria)*

*Table 4: Averaged amount of active microwave observations per (high peaking) channel over a month (February 2022).*

*Table 5: Adjustment of the conditions for microwave data assimilation in the OSSE*

*Table 6: Specified first-guess observation errors specified in AROME-Arctic for the perturbation and assimilation of EPS-Sterna data (after calibration).*

*Table 7: Sum of active EPS-Sterna observations per assimilation window and ratio between the 2 configurations (OP3-6SAT and OP3-3SAT).*

*Figure 1: The AROME-Arctic domain (upper rectangle) together with the MetCoOp EPS domain*

*Figure 2: a) Average number of active observations in AROME-Arctic for each assimilation cycle (10 days averaged number of actively assimilated observations) and b) absolute Degree of Freedom for Signal (DFS) for each observation type (averaged over 4 distant assimilation time), (Randriamampianina et al, 2019).*

*Figure 3: Difference in mean RMSE, normalized by the mean scores for 12- and 48-hr forecasts of specific humidity, between the 2 experiments in which all observations are used and various experiments in which conventional and satellite observations are denied from the regional DA. The impact of microwave (MW) observations, Humidity channels (MH) or Temperature channels (MT) through regional (REG, left panel) DA or through lateral boundary conditions (LBC, right panel) is thus shown in per cent (e.g., from -12 to 12%). Negative/positive values indicate positive/negative impact of observations on forecast skill. A 90% two-sided statistical significance test is applied, and verification is against the eight radiosonde stations in the AROME-Arctic domain. More details can be found in Randriamampianina et al, 2021.*

*Figure 4: Average number of active satellite observations in AROME-Arctic for each assimilation cycle (10 days averaged number of actively assimilated observations)*

*Figure 5: Example of EPS-Sterna coverage over Arctic for the 3 configurations (6SAT in red, 4SAT in blue and 3SAT in green) for the assimilation window of 15 UTC (+/-1 hour and 30 minutes).*

*Figure 6: Sterna weighting function assuming a standard atmosphere, applicable this study of EPS-Sterna.*

*Figure 7: Organisation of the Observing System Simulation Experiment*

*Figure 8: Example of the surface temperature field extracted from the Nature Run and interpolated on the AROME-Arctic domain on the 10/02/2022 at 06 UTC.*

Figure 9: Example coverage of existing (high peaking) passive microwave sounding data used in the assimilation in the AROME-Arctic domain, on 14 February 2022: MHS (blue), AMSU-A (yellow), MWHS-2 (orange) and ATMS (green).

Figure 10: Specified observation errors in AROME-Arctic for microwave instruments (before calibration)

Figure 11: Frequency histograms of analysis departures to observations (in K) at AMSU-A channel 8 and 9 using different scenarios of observation errors. Oper refers to the “real world” settings. osse0p2, osse0p5 and osse0.7 refer to SIGMAO\_COEFF at 0.2, 0.5 and 0.7 respectively.

Figure 12: Maps of first guess departure to MHS channel 3 observations in the “real world” (upper line) compared to those from the uncalibrated (bottom, left panel) and calibrated (bottom, right panel) “simulated world”.

Figure 13: First guess departure statistics (standard deviation and absolute average difference) per channel in the “simulated world” before and after calibration and in the “real world” for ATMS active observations. Statistics covers 15 days.

Figure 14: Specified observation errors in AROME-Arctic for microwave instruments, including a first guess for EPS-Sterna data (after calibration)

Figure 15: Example of available passes and thinking procedure of EPS-Sterna constellation at 06 UTC. Upper panel: Available observations. Lower panel: Assimilated observations from each of the passes.

Figure 16: The total observation coverage for assimilation based on the passes shown in Figure 15.

Figure 17: 5 days-accumulated EPS-Sterna active observations per assimilation window and per platform for the 3 configurations (OP3-6SAT, OP2-4SAT and OP3-3SAT). The same result is presented for MHS active data as reference.

Figure 18: Map of active observations from microwave sensors and EPS-Sterna (OP3-6SAT) on the 12/02 at 06 UTC

Figure 19: Map of active observations from microwave sensors and EPS-Sterna (upper line: OP3-6SAT, middle: OP2-4SAT and lower line: OP3-3SAT) on the 11/02 at 09 UTC.

Figure 20: Relative impact expressed as degrees of freedom for signal (DFS) per observation of EPS-Sterna at 03 (left panel) and 06 (right panel) UTC over AROME-Arctic domain. The numbers below show the total number of observations for each observation type.

Figure 21: As for Fig. 20, but for times 09 and 15 UTC.

Figure 22: Total percentage contribution of each observation type in the atmospheric analysis over 7 days (20-27/02)

Figure 23: Total percentage contribution of microwave observation types and radiosondes (TEMP as reference) in each 3h-atmospheric analysis averaged over 7 days (20-27/02)

Figure 24: Impact of the OP3-6SAT EPS-Sterna constellation. The curves show bias (dotted lines) and standard deviation (solid lines) of the departures from the Nature Run. Red curve: The control run without EPS-Sterna. Blue curves: The run with a OP3-SAT EPS-Sterna constellation added on top of the observing system of the control run. The panels (from left to right) are for temperature, specific humidity, zonal and meridional components of wind, respectively.

Figure 25: Time series of the bias and standard deviation of the departures from the Nature Run at 550 hPa, which is around where we see the maximum impact, for the same quantities as in Fig. 7.

Figure 26: The figure shows the impact of OP3-6SAT (upper line), OP2-4SAT (middle line) and OP3-3SAT (lower line) over AROME-Arctic domain expressed in terms of relative change (%) in forecast error (root-mean-square error) compared to the Nature Run. Red shadings indicate degradation, blue indicate improvements. The black line areas indicate that the improvement is significant with 95% confidence level. From left to right, each panel shows results for temperature, specific humidity, zonal and wind components.

Figure 27: Difference in mean root-mean-square error (RMSE), normalized by the mean scores, of 6- and 12-hr forecast for temperature between one experiment in which all observations are used in LBC and one experiment in which conventional observations are denied from the regional DA. The impact of all conventional observations through regional DA is shown. Negative/positive values indicate positive/negative impact of observations on forecast skill. A 90% two-sided statistical significance test is applied, and verification is against the eight radiosonde stations in the AROME-Arctic domain (Randriamampianina et al, 2021).

Figure 28: Relative difference (in %) of MTEN at 00 UTC and 12 UTC for the 3 constellation scenarios compared to the CTL where no EPS-Sterna have been assimilated (upper line). The ratio between the 2 degraded scenario and OP3-6SAT is also presented (lower line). The diagnostic has been run for the period from 20 to 27th of February 2023.

Figure 29: Relative difference in the standard deviation (in %) of analysed specific humidity versus the Nature Run at each assimilation time (00, 03, 06, 12, 15, 18 and 21 UTC) for the OP3-6SAT in blue and OP3-3SAT in green constellation scenario and the No Metop-B experiment in grey compared to the CTL in red. No EPS-Sterna have been assimilated in the denial nor the control run. Negative/positive values indicate positive/negative impact of observations on forecast skill. The statistics have been run for the 15th of February 2023.

Figure 30: Same as 29 but for the 3h-forecast.

Figure 31: Same as 29 but for the 24 h-forecast (valid at the analysis of 15th of February).

Figure 32: Relative difference in the standard deviation (in %) of analysis (left panel), 6h-forecast (middle panel) and 12h-forecast (right panel) of temperature versus the Nature Run. Forecast is based on the analysis of 00 UTC.

Figure 33: 5-days accumulated precipitation (rain+snow+graupel) over the AROME-Arctic domain as analysed in the experiments with EPS-Sterna OP3-6SAT and OP2-4SAT, in the CTL (without EPS-Sterna) and in the Nature Run. Data covers the period from 10 to 15th of February 2022.

Figure 34: Maps of active EPS-Sterna observations in OP3-6SAT configuration on the 15/02 at 12UTC.

Figure 35: Maps of precipitation as produced in the Nature Run on the 16/02 at 00UTC compared to 12h-forecast valid on the 16/02-00h based on the analysis of the 15/02 at 12UTC from the OP3-6SAT configuration and the CTL.

## References

Bengtsson, L., et al, 2017: The HARMONIE–AROME Model Configuration in the ALADIN–HIRLAM NWP System. *Mon. Wea. Rev.*, 145, 1919–1935, <https://doi.org/10.1175/MWR-D-16-0417.1>.

Chapnik, B.; Desroziers, G.; Rabier, F.; Talagrand, O., 2006: Diagnosis and tuning of observational error in a quasi-operational data assimilation setting. *Q. J. R. Meteorol. Soc.* 2006, 132, 543–565.

Dahlgren, P., 2023: Impact of satellite data in a regional reanalysis system, ITSC-24, [https://itwg.ssec.wisc.edu/wordpress/wp-content/uploads/2023/05/oral.15.06.dahlgren\\_itsc24.pdf](https://itwg.ssec.wisc.edu/wordpress/wp-content/uploads/2023/05/oral.15.06.dahlgren_itsc24.pdf)

Denis, B., R. Laprise, D. Caya, J. Côté, 2002. Downscaling ability of one-way nested regional climate models: the big-brother experiment. *Climate Dynamics*, 18, 627-646. doi 10.1007/s00382-001-0201-0.

Errico, R.M., and D.P. Baumhefner, 1987: Predictability experiments using a high-resolution limited-area model. *Mon. Wea. Rev.*, 115, 488-504.

Fisher, M., 2003: Estimation of Entropy reduction and Degrees of freedom for signal for large variational analysis systems, ECMWF Technical Memoranda, 397, 2003. DoI 10.21957/2bec9m38o . Available on <https://www.ecmwf.int/en/elibrary/74482-estimation-entropy-reduction-and-degrees-freedom-signal-large-variational> .

Karbou, F., E. Gérard, and F. Rabier, 2006, Microwave Land Emissivity and Skin Temperature for AMSU-A & -B Assimilation Over Land, *Q. J. R. Meteorol. Soc.*, vol. 132, No. 620, Part A, pp. 2333-2355(23).

Lawrence, H, Bormann, N, Sandu, I, Day, J, Farnan, J, Bauer, P. Use and impact of Arctic observations in the ECMWF Numerical Weather Prediction system. *Q J R Meteorol Soc.* 2019; 145: 3432– 3454. <https://doi.org/10.1002/qj.3628>

Q. Liu, F. Weng and S. J. English, "An Improved Fast Microwave Water Emissivity Model," in IEEE Transactions on Geoscience and Remote Sensing, vol. 49, no. 4, pp. 1238-1250, April 2011, doi: 10.1109/TGRS.2010.2064779.

Masson, V., et al. "The SURFEXv7. 2 land and ocean surface platform for coupled or offline simulation of earth surface variables and fluxes." Geoscientific Model Development 6.4 (2013): 929-960

Masutani, M. et al., 2010: Observing System Simulation Experiments. In: Lahoz, W., Khattatov, B., Menard, R. (eds) Data Assimilation. Springer, Berlin, Heidelberg.  
[https://doi.org/10.1007/978-3-540-74703-1\\_24](https://doi.org/10.1007/978-3-540-74703-1_24).

Müller, M., Y. Batrak, J. Kristiansen, M.A. Køltzow, G. Noer, and A. Korosov, 2017: Characteristics of a Convective-Scale Weather Forecasting System for the European Arctic. Mon. Wea. Rev., 145, 4771–4787, <https://doi.org/10.1175/MWR-D-17-0194.1>.

Rabier, F., Fourrié, N., Chafaï, D., and Prunet, P., 2002: Channel selection methods for infrared atmospheric sounding interferometer radiances. Quart. J. Roy. Meteor. Soc., 128, 1011-1027.

Randriamampianina R, Schyberg H, Mile M., 2019: Observing System Experiments with an Arctic Mesoscale Numerical Weather Prediction Model. Remote Sensing, 2019; 11(8):981.  
<https://doi.org/10.3390/rs11080981>

Randriamampianina, R, Bormann, N, Køltzow, MAØ, Lawrence, H, Sandu, I, Wang, Z. Relative impact of observations on a regional Arctic numerical weather prediction system. Q J R Meteorol Soc. 2021; 147: 2212– 2232. <https://doi.org/10.1002/qj.4018>

Storto, A. and Randriamampianina, R. (2010) The relative impact of meteorological observations in the Norwegian regional model as determined using an energy norm-based approach. Atmospheric Science Letters, 11, 51– 58.

Weng, F., Yan, B., and Grody, N. C. (2001), A microwave land emissivity model, J. Geophys. Res., 106( D17), 20115– 20123, doi:10.1029/2001JD900019.

Zeng, X., and Coauthors, 2020: Use of Observing System Simulation Experiments in the United States. Bull. Amer. Meteor. Soc., 101, E1427–E1438, <https://doi.org/10.1175/BAMS-D-19-0155.1>.